Title	Engineering and Braiding Non-Abelian Anyons in Topological Superconducting Systems
Author(s)	三野, 巧
Citation	大阪大学, 2023, 博士論文
Version Type	VoR
URL	https://doi.org/10.18910/92217
rights	
Note	

Engineering and Braiding Non-Abelian Anyons in Topological Superconducting Systems

TAKUMI SANNO

MARCH 2023

Engineering and Braiding Non-Abelian Anyons in Topological Superconducting Systems

A disseration submitted to
THE GRADUATE SCHOOL OF ENGINEERING SCIENCE
OSAKA UNIVERSITY
in partial fulfillment of the requirements for the degree of
DOCTOR OF PHILOSOPHY IN SCIENCE

BY

TAKUMI SANNO

MARCH 2023

Abstract

Quantum many-body systems generate elegant and exotic physical phenomena, which always ask us the elementary principles of phenomena that emerged in many-body systems. Although it is difficult to understand all structures of quantum many-body systems, much has steadily become clear through both theoretical and experimental work. In the last two decades, topological systems have been the main topics of quantum many-body systems. Topological systems are characterized by topological numbers that could be defined by bulk symmetries. This topological number does not change without closing the energy gap. Thus, topological systems could be realized robust against local perturbations. Moreover, these systems have exotic quasiparticle excitations which obey unconventional quantum statistics different from bosons and fermions. For these statistics, a state gets an overall phase factor that takes any value. In being named after this exotic property, these quasiparticles are called anyon. In the case where the state is degenerate, this phase factor will become a matrix, which implies that the final state depends on the exchange order of anyons. These anyons (statistics) are called non-Abelian anyons (statistics). One candidate of non-Abelian anyons is a Majorana quasiparticle that emerged in fractional Hall states, topological superconductors, and Kitaev materials. Recent experimental works support the presence of Majorana quasiparticles. In addition, to catch the tail of Majorana quasiparticles, there are some crucial issues, such as realizing the Majorana many-body problem, seeking other exotic quasiparticles in topological materials, and implementing topological quantum computation.

Now, the classification of topological phases is generalized to non-Hermitian systems. Some of these phases can be adiabatically deformed into topological phases of Hermitian systems, while there are some topological phases that cannot be deformed into that. The latter topological phases are called non-Hermitian topological phases, and these phases show phenomena specific to non-Hermite systems.

In this thesis, we explore physics that emerged from the collaboration of the Majorana many-body systems and non-Hermitian characters. A non-Hermitian character would enrich the phase diagrams of the Majorana many-body systems and then lead to the development of the non-Abelian anyons. We propose non-Hermitian Majorana interacting systems that can be the platform of Yang-Lee anyons. Yang-Lee anyons are described by the non-unitary conformal field theory with the central charge $c = -22/5$ and might have the potential for simulating non-equilibrium dynamics of open quantum systems. Moreover, we present a scheme for fusion, measurement, and braiding in our designed systems.

Contents

Chapter 1

Introduction

Statistics play an essential role as *Holy Grail* in quantum physics. Classical particles are always distinguishable, and then we can track the *shadow* of them at all times. For quantum physics, we, of course, can experimentally detect the position of a particle through a spatially extended wave function. However, this wave function of particles would overlap, even if their peaks are not at identical positions. It is impossible to define distinguishable particles in a basic process, which means the *indistinguishability* of particles. Thus, these consequences make us adopt the notion of statistical physics, considering the indistinguishable particles. In three spatial dimensions, particles generally come into two conventional species: bosons and fermions. Bosons satisfy the Bose-Einstein statistics, and fermions do the Fermi-Dirac statistics. These properties of particles can be obtained from the results through experiments, which is well known as the *elementary principle* of modern physics, such as superconductivity, quantum electrodynamics, and so on.

In two spatial dimensions, the wave functions of particles satisfy the non-trivial statistics to realize the notion of anyons. Anyons are exotic particles that obey unconventional quantum statistics different from fermions and bosons [1], and emerge as fractionalized quasiparticles in topological phases of two-dimensional systems such as fractional quantum Hall (FQH) states [2, 3, 4], topological superconductors (TSC) [5, 6], and quantum spin liquids (QSL) [7]. In the last two decades, the application of anyons to fault-tolerant quantum computation, which is referred to as topological quantum computation [7, 8, 9, 10, 11, 12, 13, 14, 15, 16, 17, 18, 19, 20, 21, 22, 23, 24, 25], has been extensively studied. In this scheme, information is stored as topological charges of anyons in a non-local way and is protected from environmental perturbations. Quantum gates necessary for computation are implemented via the exchange of spatial positions (braiding) of anyons. In particular, *non-Abelian* *anyons* for which the braiding operations are non-commutative unitary operations acting on a topologically degenerate ground state of many anyon systems are quite useful for the realization of universal topological quantum computation [7, 10]. One possible candidate of non-Abelian anyons for this purpose is a Majorana bound state of a topological superconductor [6, 11, 12, 13, 14, 17, 18, 19, 20, 21, 22, 23, 24, 25, 26, 27, 28, 29, 30, 31, 32, 33, 34]. Moreover, Majorana many-body systems have rich phase diagrams. Recent studies proposed that strongly correlated Majorana systems can exhibit novel phenomena, such as emergent spacetime supersymmetry, topological order, quantum chaos, and black holes. [35, 36, 37, 38, 39, 40]. Another possible candidate of non-Abelian anyons is the Fibonacci anyon [8, 41]. This anyon can be described by the Wess-Zumino-Witten Conformal Field Theory with the central charge $c = 14/5$ and enable us to realize universal topological quantum computation. These are several systems with Fibonacci anyons: the Read-Rezayi FQH state [42, 43], superconductor-FQH junction systems [44], a septuplt-layer topological superconductor [37], and a Rydberg atom gas [45]. We easily find that topological phases contribute significantly to condensed matter physics. Recently, topological phases in non-equilibrium open systems have attracted a great deal of attention. These systems are effectively described by the non-Hermitian Hamiltonian [46]. Recent studies reveal phenomena specific to non-Hermitian systems [47, 48, 49]. Moreover, the fundamental principle of symmetry in non-Hermitian topological phases is well established [50].

Fibonacci anyon has the potential of universal topological quantum computation. However, it is challenging to realize these proposed systems experimentally. In this thesis, we propose and design the non-Hermitian Majorana systems that can be realized as the Yang-Lee model. The Yang-Lee model is the transverse Ising model under an imaginary magnetic field ih and possesses the parity-time $\mathcal{PT}$ symmetry. Also, this model has the exotic quasiparticle, called Yang-Lee anyon, at the critical point where it shows the $\mathcal{PT}$ symmetry breaking. Yang-Lee anyons are described by the nonunitary conformal field theory with the central charge $c = -22/5$, and are nonunitary counterparts of Fibonacci anyons, obeying the same fusion rule but exhibiting nonunitary non-Abelian braiding statistics. We consider a topological superconductor junction system coupled with dissipative electron baths, which realizes a non-Hermitian interacting Majorana system. On the basis of this scenario, we present a scheme for the fusion, measurement, and braiding of Yang-Lee anyons in our proposed setup. This thesis is structured as follows:

- In Chap.2, we briefly introduce the elementary notion of Abelian and non-Abelian anyons. In particular, non-Abelian anyons obey unconventional quantum statistics that the operator of exchanging anyons is not commutative. Also, these features apply to quantum computation that can encode information non-locally. Generally, the mathematical aspect is described by the fusion tensor category, which is not easily accessible to standard physicists. Thus, we focus on three non-Abelian anyons: Ising anyons, Fibonacci anyons, and Yang-Lee anyons.

- In Chap.3, we overview the conformal field theory(CFT). CFT is an effective theory to identify systems with anyons. In CFT, systems possess conformal symmetry with Lorentz invariance and local scale invariance. This theory would describe critical phenomena well and give us the universality class of systems. In particular, we discuss the specific models corresponding to Ising anyons and Yang-Lee anyons.
- In Chap.4, we propose non-Hermitian Majorana systems that can enrich phase diagrams of Majorana systems and lead to realizing the features of Majorana quasiparticles. Our designed system is 1D TSC junction systems coupling with electron baths and can be realized as the Yang-Lee model in spin systems. By controlling coupling constants between TSCs and electron baths, this system can host the Yang-Lee anyons at critical points. Also, we numerically estimate the Yang-Lee criticality against a single Majorana hopping term that would be an inevitable term.
- In Chap.5, we summarize this thesis on non-Hermitian Majorana systems.

Chapter 2

Introduction to Abelian and Non-Abelian Anyons

Anyons are exotic particles that obey unconventional quantum statistics different from bosons and fermions[1]. In particular, non-Abelian anyons have the potential for the application of fault-tolerant quantum computation. Braiding operations, exchanging of two anyons, can construct quantum gates, which are topologically protected from local perturbations.

Majorana bound states in TSC is the candidate of non-Abelian anyons. However, the braiding operators of Majorana bound states are not sufficient for the construction of universal quantum gates. More promising candidates are Fibonacci anyons, which enable us to realize universal topological quantum computation only via topologically protected braiding manipulations [10, 41, 51, 52]. Recent studies proposed condensed matter systems where Fibonacci anyons appear; the Read-Rezayi FQH state [42, 43], superconductor-FQH junction systems[44], a septuple-layer topological superconductor [37], and a Rydberg atom gas [45]. Also, there is a close cousin of Fibonacci anyon realizable in a non-Hermitian quantum system, and this non-Abelian anyon is called Yang-Lee anyon [53, 54]. Yang-Lee anyons obey the same fusion algebra as Fibonacci anyons and might have computational power comparable to Fibonacci anyons.

2.1 Abelian and Non-Abelian Anyons

First of all, we would like to discuss the Abelian and non-Abelian statistics. These statistics only appear in the two dimensions, which can be easily realized through a loop of one moving particle around another particle. Also, we introduce the characteristic features of anyons, such as the fusion rule, F-symbol, and R-matrix. The braiding operators are derived from these features. Next, we would like to discuss examples of non-Abelian anyons. We briefly introduce the explicit form of the fusion rule, F-symbol, and R-matrix. Also, we discuss the candidate systems hosting non-Abelian anyons, such as topological superconductors.

2.1.1 Abelian and Non-Abelian Statistics

Abelian and non-Abelian statistics can be easily realized through the schematic of a loop of one moving particle around another particle [55]. Fig. 2.1 shows the loop

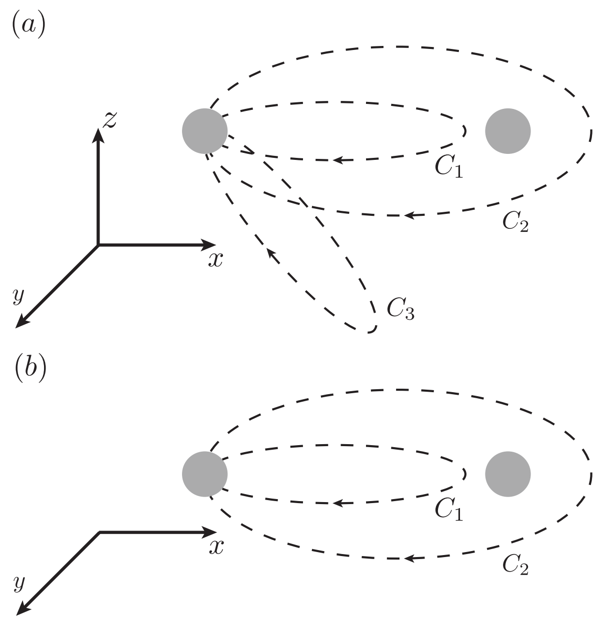

Figure 2.1: Schematic of exchanging particles in two and three dimensions.

of two and three dimensions. Let us consider the wave function $\psi(C_i)$ depending on the path C_i. As seen in Fig. 2.1(a), there are three paths $C_i (i = 1, 2, 3)$ in three dimensions, and we can deform one path to other paths continuously. This result implies that these paths are the topologically same path, which means that the wave functions $\psi(C_i)$ in three dimensions satisfy

$$\psi(C_1) = \psi(C_2) = \psi(C_3). \tag{2.1}$$

Also, twice the exchange of two particles is equivalent to the loop in Fig.2.1(a). Thus, the overall phase factor $e^{i\varphi}$ of an exchange of two particles satisfies $e^{i2\varphi} = 1$.

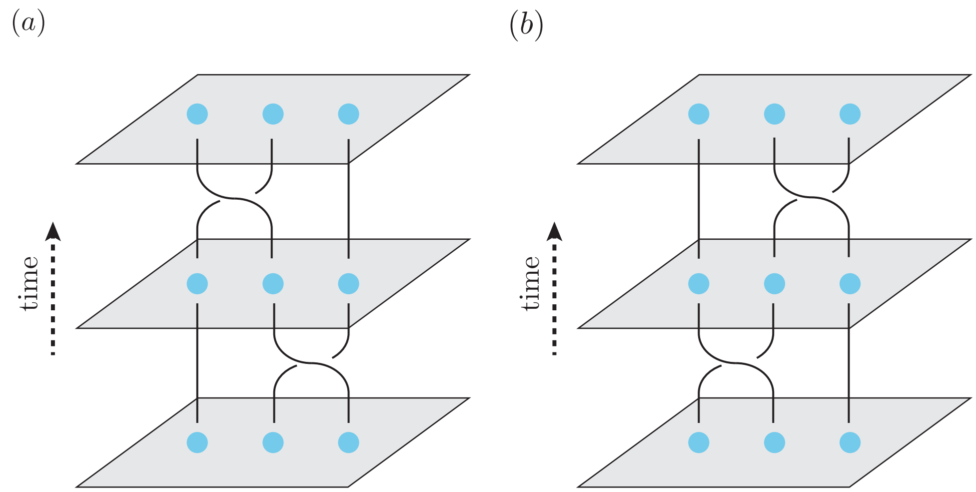

Figure 2.2: Schematic of Braiding

This phase factor has two type : $\varphi = 0$ (bosonic statistics) and $\varphi = \pi$ (fermionic statistics).

For two dimensions, statistics come into four species: bosons, fermions, Abelian anyons, and non-Abelian anyons. As seen in Fig. 2.1(b), there are two paths $C_i(i = 1, 2)$ in two dimensions, and we can not continuously deform the path $C_1(C_2)$ to the path $C_2(C_1)$ respectively. This result implies that the two paths are topologically distinct. Thus, it is possible that the overall phase factor $e^{i\varphi}$ takes any value. This exotic particle with any phase factor is called an *anyon*[1]. Moreover, we would like to consider the degenerate case. In this case, the overall phase factor would be more complicated and become a matrix. Generally, a matrix does not commute each other (non-Abelian), which means that the final state depends on the exchange order (Fig. 2.2). These exotic statistics are called *non-Abelian statistics* and are well known as the Braid group in mathematics, and then the exchange operator is called a *Braiding* operator.

The braiding rules for Abelian (non-Abelian) statistics are derived from three important factors; the fusion rule, the F-symbol, and the R-matrix. The fusion rule means the process that multiplying two anyons can construct other anyons in Fig. 2.3(a) and then is the basic notion of understanding the physics of anyons. The F-symbol is a matrix for the transformation between different fusion bases, which is expressed as shown in Fig. 2.3(b). The braidings of two anyons are described by

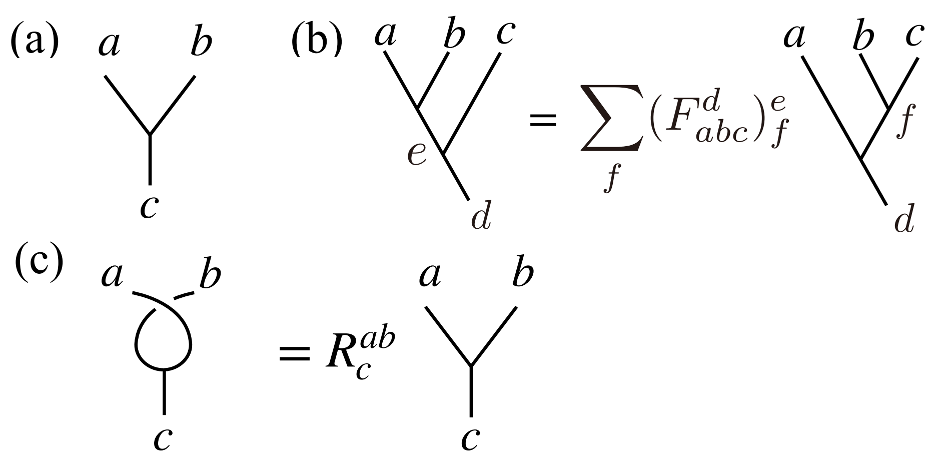

Figure 2.3: (a) Diagrammatic expression of the fusion rule. $a, b, c, \ldots$ denote a state with an anyon. (b) Diagrammatic expression of the F-symbol. (c) Diagrammatic expression of the R-matrix.

the R-matrix R^{ab}_c, which transposes two anyons a and b fusing into an anyon c. The diagrammatic expression of the R-matrix is shown in Fig. 2.3(c). Also, this matrix is obtained from the topological spin, which describes the phase change arising from the braiding of two anyons, combined with the hexagon equation satisfied by the F-symbol and the R-matrix.

In general, the fusion rule is given by

$$a \times b = \sum_c N^c_{ab} c, \tag{2.2}$$

where a, b, c are particles and N^c_{ab} is an non-negative integer. For Abelian anyons, there is one type anyon c with $N^c_{ab} = 1$ and all other c with $N^c_{ab} = 0$. The toric code model is an example of Abelian anyons [56]. In this model, there are four type particles $\mathbb{I}, e, m, \epsilon$, where $\mathbb{I}$ means the vacuum, and the fusion rules are as follows

$$\begin{gathered} e \times e = \mathbb{I},\ m \times m = \mathbb{I},\ \epsilon \times \epsilon = \mathbb{I}, \\ e \times m = \epsilon,\ e \times \epsilon = m,\ m \times \epsilon = e, \end{gathered} \tag{2.3}$$

and then these anyons obey the Abelian statistics.

2.1.2 Topological Quantum Computation

Let us talk about the application of anyons, such as topological quantum computation. Quasiparticles in topological systems satisfy the characteristic features of anyons. Topological systems have these origins in the fractional quantum hall effect and denote the topological insulator, topological superconductor, topological superfluid, and Kitaev materials. Also, these systems are classified with the topological number, take an integer value, determined by bulk symmetries such as time-reversal symmetry, particle-hole symmetry, chiral symmetry, and so on [57]. In general, this topological number does not change without closing the energy gap. Thus, topological systems can be realized robust against local perturbations. For the systems with the non-zero topological number, these systems can host the zero-energy quasiparticles at the interface, which is called *bulk-edge correspondence* [58]. Of course, these quasiparticles have taken over the nature of topological systems and then are topologically protected from local perturbations.

Topological quantum computation is the quantum computation in which we can encode information to anyonic qubits non-locally [8]. As mentioned above sentence, anyons can be realized as quasiparticles in topological systems. Thus, this qubit is robust against local perturbations and does not, in principle, cause errors. Also, quantum gates can be composed of braiding operations, which implies that the final state only depends on the order of braiding operations. However, for some non-Abelian anyons, the braiding operations can not construct the universal quantum gates while these qubits are sufficiently robust against local perturbations. In this case, it is necessary to introduce a non-topological operation, the observation of anyon charge, for the construction of universal quantum gates, and the universal quantum gates are implemented as a combination of braiding operations and non-topological operations. These quantum gates would cause errors. Thus, we need to seek reasonable non-Abelian anyons or to construct the non-topological operation with sufficiently small errors.

In next section, we introduce an example of non-Abelian anyons and the implementation of topological quantum computation: to construct q-bit and qunatum gates.

2.2 Examples of Non-Abelian Anyons

Obviously, non-Abelian statistics are more complicated than Abelian statistics. Let us discuss three anyons as examples of non-Abelian anyons, such as Ising anyons, Fibonacci anyons, and Yang-Lee anyons. Ising anyons would be the most famous examples of non-Abelian anyons.

2.2.1 Ising Anyons

First of all, we would like to discuss the Ising anyons. There are three particle types: the vacuum $\mathbb{I}$, the non-Abelian anyon σ, and fermion ψ. The fusion rules are given by

$$\sigma \times \sigma = \mathbb{I} + \psi, \ \sigma \times \psi = \sigma, \ \psi \times \psi = \mathbb{I}. \tag{2.4}$$

The first fusion rule implies that σ anyon is its own antiparticle, and the fusion of two σ anyons means that these anyons would annihilate or the creation of the fermion ψ. The second fusion rule means that σ anyon can absorb the fermion ψ without changing its anyonic charge. An anyonic charge specifies whether a particle is equivalent to the vacuum, the boson, the fermion, and the anyon. We can only observe the fermion parity, the parity of the total fermion number because the fusion of two fermions ψ is to be the vacuum.

The explicit forms of F-symbol and R-matrix are given by

$$F^{\sigma}_{\sigma\sigma\sigma} = \frac{1}{\sqrt{2}}\begin{pmatrix} 1 & 1 \\ 1 & -1 \end{pmatrix}, \ R^{\sigma\sigma} = e^{-i\pi/8}\begin{pmatrix} 1 & 0 \\ 0 & i \end{pmatrix}, \tag{2.5}$$

where the basis of these matrix is spanned by the states $|\mathbb{I}\rangle, |\psi\rangle$. These explicit forms can be obtained by the pentagon and hexagon indentities [59]. The pentagon identity represents two distinct fusion processes of four anyons with a fixed final state. Also, the hexagon identity represents two distinct fusion processes of three anyons with a fixed final state. From the R-matrix, we found that a fermion ψ gains an additional phase $\pi/2$ compared to the vacuum state. Braiding is the exchange of two anyons σ, and then this operation does not change the fermion parity of the system. Thus, the application of the quantum computation requires four anyons σ that can construct the four states $|\mathbb{I}\rangle \otimes |\mathbb{I}\rangle, |\psi\rangle \otimes |\mathbb{I}\rangle, |\mathbb{I}\rangle \otimes |\psi\rangle, |\psi\rangle \otimes |\psi\rangle$.

Let us consider the topological superconducting systems as an example of the application to topological quantum computation. Majorana bound states γ satisfy the features of Ising anyons and that of Majorana fermion, which is a self-Hermitian particle [60, 61]. Majorana bound states would emerge at defects in topological superconductors (TSC) such as the core of vortices and edges [62, 63]. Recent studies have revealed that Majorana bound states can be induced in several systems: s-wave superconductors with Rashba spin-orbit coupling [64, 65, 66], superconducting nanowires [31, 33], Fu-Kane model [67], and iron-based superconductor Fe(Se,Te) [68, 69].

We would like to discuss the topological quantum computation (TQC) of Majorana bound states. The implementation of universal quantum computation needs some sets of quantum gates; phase gate S, Hadamard gate H, T-gate ($\pi/8$ gate), and CNOT gate. CNOT gate is only a two-qubit gate. Braidings of Majorana bound states can implement phase gate S, Hadamard gate H, and CNOT gate, while T-gate can not realize as the braiding of them. To implement T-gate, we need non-topological operations where Majorana bound states are moved closer to or far away from each other. This operation, however, involves errors that violate advantages such as topological quantum computation. Recent studies of these systems focus on the implementation of universal quantum computation [11, 70].

Now, we consider the systems hosting $2N$ Majorana bound states γ_j. Majorana bound states γ_j satisfy following conditions

$$\gamma_j = \gamma_j^\dagger,\ \gamma_j^2 = 1, \{\gamma_i, \gamma_j\} = 0.$$

First of all, we would like to construct the Hilbert space. We can define a non-local complex fermion ψ_j as $\psi_j \equiv (\gamma_{2j-1} + i\gamma_{2j})/2$, the number operator n_j as

$$n_j \equiv \psi_j^\dagger \psi_j = \frac{1}{2}\left(1 + i\gamma_{2j-1}\gamma_{2j}\right), \tag{2.6}$$

which leads to a total degeneracy 2^N. This degeneracy is called a *topological degeneracy* and can not be split by local perturbations. Moreover, in superconducting systems, the fermion parity P,

$$P \equiv \prod_j i\gamma_{2j-1}\gamma_{2j}, \tag{2.7}$$

must be conserved, which implies that this degeneracy is reduced to 2^{N-1} for each parity sector. In general, under the Braiding of γ_i and γ_j, Majorana bound states γ_i, γ_j would transform as $\gamma_i \to \gamma_j,\ \gamma_j \to -\gamma_i$ since the fermon parity P is conserved. Thus, the explicit forms of the Braiding can be defined as

$$B_{i,j} \equiv \exp\left[-\frac{\pi}{4}\gamma_i\gamma_j\right] = \frac{1}{\sqrt{2}}\left[1 - \gamma_i\gamma_j\right]. \tag{2.8}$$

We would like to construct some quantum gates by using braidings of Majorana bound states. An important property is that three Majorana bound states $\gamma_1, \gamma_2, \gamma_3$ constitute the Pauli matrices as

$$-i\gamma_1\gamma_2 = \sigma_z, -i\gamma_2\gamma_3 = \sigma_x, -i\gamma_3\gamma_1 = \sigma_y. \tag{2.9}$$

From this relation, some one-qubit quantum gates can be described by braiding operations as

$$\text{Phase gate S: } S = B_{1,2} = e^{-i\frac{\pi}{4}} \begin{pmatrix} 1 & 0 \\ 0 & i \end{pmatrix}, \tag{2.10}$$

$$\text{Hadamard gate H: } H = (B_{2,3})^2 B_{3,1} = \frac{-i}{\sqrt{2}} \begin{pmatrix} 1 & 1 \\ 1 & -1 \end{pmatrix}, \tag{2.11}$$

$$\text{NOT gate: NOT} = (B_{2,3})^2 = -i \begin{pmatrix} 0 & 1 \\ 1 & 0 \end{pmatrix}. \tag{2.12}$$

Next, we consider two Majorana qubits. CNOT gate can be described by Majorana bound states γ_j as

$$\begin{aligned} \text{CNOT} \equiv \begin{pmatrix} \mathbb{I} & 0 \\ 0 & \sigma_x \end{pmatrix} &= \begin{pmatrix} H & 0 \\ 0 & H \end{pmatrix} \begin{pmatrix} \mathbb{I} & 0 \\ 0 & \sigma_z \end{pmatrix} \begin{pmatrix} H^\dagger & 0 \\ 0 & H^\dagger \end{pmatrix} \\ &= e^{i\frac{\pi}{4}} \begin{pmatrix} H & 0 \\ 0 & H \end{pmatrix} \exp\left[-i\frac{\pi}{4}\gamma_1\gamma_2\gamma_5\gamma_6\right] B_{1,2}B_{5,6} \begin{pmatrix} H^\dagger & 0 \\ 0 & H^\dagger \end{pmatrix}. \end{aligned} \tag{2.13}$$

To realize $\exp\left[-i\frac{\pi}{4}\gamma_1\gamma_2\gamma_5\gamma_6\right]$, we need to the ancillary Majorana bound states γ_9, γ_{10} and prepare the state $|\varphi\rangle$ satisfying $\psi_{9,10}|\varphi\rangle = 0$ [11, 12]. Acting this operation on the preparing state $|\varphi\rangle$, we obtain

$$\exp\left[-i\frac{\pi}{4}\gamma_1\gamma_2\gamma_5\gamma_6\right]|\varphi\rangle = 2B_{10,6}\Pi_+^2\Pi_+^4|\varphi\rangle = 2B_{6,10}\Pi_-^2\Pi_-^4|\varphi\rangle, \tag{2.14}$$

where we define projection operations $\Pi_\pm^2, \Pi_\pm^4$ as $\Pi_\pm^2 \equiv \frac{1}{2}(1 \mp i\gamma_6\gamma_9), \Pi_\pm^4 \equiv \frac{1}{4}(1 \pm \gamma_1\gamma_2\gamma_5\gamma_9)$. Thus, the operation $\exp\left[-i\frac{\pi}{4}\gamma_1\gamma_2\gamma_5\gamma_6\right]$ can be realized as the measurement of $-i\gamma_6\gamma_9$ and $-\gamma_1\gamma_2\gamma_5\gamma_9$ and braiding $B_{10,6}$. Finally, we construct T-gate which is a non-topologically protected operation. Let us consider the target state, $|\psi\rangle = \alpha|0\rangle + \beta|1\rangle$, and the ancillary state, $|\varphi\rangle = \frac{1}{\sqrt{2}}(|0\rangle + e^{i\frac{\pi}{4}}|1\rangle)$. T-gate is composed of two steps: (i) acting CNOT gate on the state $|\psi\rangle \otimes |\varphi\rangle$ and (ii) the measurement of the ancillary state $|\varphi\rangle$. If we measured $|1\rangle$ on step (ii), we should apply the phase gate to the target state. Step (i) is

$$|\psi\rangle \otimes |\varphi\rangle \xrightarrow[\text{CNOT}]{} \frac{\alpha}{\sqrt{2}}|0\rangle \otimes (|0\rangle + e^{i\frac{\pi}{4}}|1\rangle) + \frac{\beta}{\sqrt{2}}|1\rangle \otimes (e^{i\frac{\pi}{4}}|0\rangle + |1\rangle). \tag{2.15}$$

Step (ii) is the measurement of the ancillary state $|\varphi\rangle$ in Eq. (2.15). If $|\varphi\rangle = |0\rangle$, the state would be $\frac{1}{\sqrt{2}}(\alpha|0\rangle + e^{i\frac{\pi}{4}}\beta|1\rangle) \otimes |0\rangle$, which implement T-gate. On the other hand, if $|\varphi\rangle = |1\rangle$, the state would be $\frac{1}{\sqrt{2}}(e^{i\frac{\pi}{4}}\alpha|0\rangle + \beta|1\rangle)\otimes|1\rangle$ and then acting phase gate on this state we implement T-gate:

$$\frac{1}{\sqrt{2}}(e^{i\frac{\pi}{4}}\alpha|0\rangle + \beta|1\rangle)\otimes|1\rangle \xrightarrow[\text{phase gate}]{} \frac{1}{\sqrt{2}}(\alpha|0\rangle + e^{i\frac{\pi}{4}}\beta|1\rangle)\otimes|1\rangle\,. \tag{2.16}$$

The key point of T-gate is preparing the ancillary state as $\frac{1}{\sqrt{2}}(|0\rangle + e^{i\frac{\pi}{4}}|1\rangle)$. First of all, we consider the state $|\varphi\rangle = \frac{1}{\sqrt{2}}(|0\rangle + |1\rangle)$. To prepare the state, we operate the non-topological operation in which Majorana bound states are moved closer to each other. This non-topological operation is bringing γ_1 and γ_2 closer for a time $t = \frac{\pi}{8\varepsilon}$, which implies that the state can acquire the dynamical phase factor $e^{-i\varepsilon t\sigma_z}$ where we consider the effective Hamiltonian $H = i\varepsilon\gamma_1\gamma_2 = -\varepsilon\sigma_z$:

$$|\psi_0\rangle \to e^{-i\varepsilon t\sigma_z}|\psi_0\rangle = \frac{e^{-i\varepsilon t\sigma_z}}{\sqrt{2}}(|0\rangle + |1\rangle)\,. \tag{2.17}$$

After this operation, we need to return γ_1 and γ_2 to the original positions:

$$\frac{e^{-i\frac{\pi}{8}}}{\sqrt{2}}\left(|0\rangle + e^{i\frac{\pi}{4}}|1\rangle\right). \tag{2.18}$$

We have introduced the theoretical framework of quantum computation using Majorana bound states. At the end of Ising anyons, we would like to introduce the numerical studies of braiding Majorana bound states. Let us consider twice the exchange of γ_2 and γ_3. If we set the initial state as $|00\rangle$, the time-evolved state were as follows

$$|00\rangle \xrightarrow[B_{2,3}]{} \frac{1}{\sqrt{2}}(|00\rangle - i|11\rangle) \xrightarrow[B_{2,3}]{} -i|11\rangle\,. \tag{2.19}$$

These consequences imply that Majorana bound states obey the non-Abelian statistics, and the Braiding operations might correspond to quantum gates. We have numerically simulated this result, as seen in Fig. 2.4 [71]. Fig. 2.4 (c) shows the transition of the quasiparticle states under braiding Majorana bound states. These numerical results imply that twice braiding ($t = 2T$) causes the transition of the quasiparticle states: $-E_1 \to +E_2, -E_2 \to +E_1$. Thus, this braiding operation is the unitary transformation of the encoded state $|00\rangle$ to $|11\rangle \equiv \hat{\eta}^\dagger_{+E_2}\hat{\eta}^\dagger_{+E_1}|00\rangle$.
[1]

[1]There are some references for the Majorana braiding dynamics [72, 73, 74, 75].

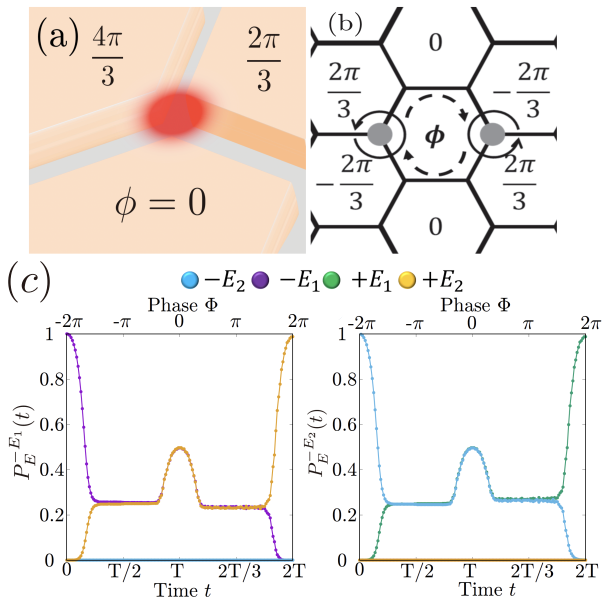

Figure 2.4: (a) Schematic of a trijunction hosting a single Majorana quasiparticle. Each superconducting island has a different phase, $\phi = 0, \pm 2\pi/3$, and the intersection is regarded as a phase singularity. (b) Schematic of the two-dimensional network of trijunctions. The braiding of Majorana bound states γ is implemented by rotating the phase ϕ from 0 to 2π. (c) Projection of the time-evoluting state $|\psi(t)\rangle$ onto the encoded state $|\varphi_{E_i}\rangle$, where E_i means the quasiparticle spectra. Twice braiding ($t = 2T$) causes the transition of the quasiparticle states: $-E_1 \to +E_2, -E_2 \to +E_1$. This result implies that twice braiding operation is equal to the unitary transformation of the encoded state $|00\rangle$ to $|11\rangle \equiv \hat{\eta}^{\dagger}_{+E_2}\hat{\eta}^{\dagger}_{+E_1}|00\rangle$.

2.2.2 Fibonacci Anyons

Next, we would like to discuss the Fibonacci anyons that are more promising for implementing the universal topological quantum computation [8, 41, 51, 76]. There are two particle types $\mathbb{I}, \tau$ in this anyonic system. The fusion rules are as follows

$$\tau \times \tau = \mathbb{I} + \tau. \tag{2.20}$$

The explicit forms of F-symbol and R-matrix for Fibonacci anyons are given by

$$F^{\tau}_{\tau\tau\tau} = \begin{pmatrix} \phi^{-1} & \phi^{-1/2} \\ \phi^{-1/2} & -\phi^{-1} \end{pmatrix}, R^{\tau\tau} = \begin{pmatrix} e^{i\frac{4}{5}\pi} & 0 \\ 0 & -e^{i\frac{2}{5}\pi} \end{pmatrix}, \tag{2.21}$$

where $\phi = (1+\sqrt{5})/2$ is the golden mean [77]. Here, the F-symbol acts on the two-dimensional space spanned by the trivial vacuum state $\mathbb{I}$ and the non-trivial state with a Fibonacci anyon τ. Now, we consider the three state $|0\rangle, |1\rangle$ and $|N\rangle$ depicted

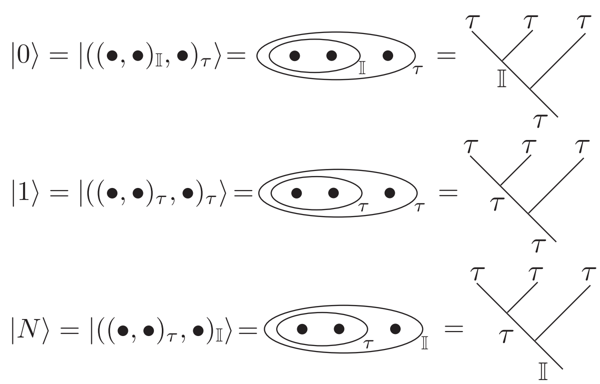

Figure 2.5: The three state $|0\rangle, |1\rangle, |N\rangle$ of three Fibonacci anyons $\bullet$.

in Fig. 2.5 [8]. The two states $|0\rangle$ and $|1\rangle$ are utilized as qubits for the application of quantum computation. The state $|N\rangle$ is a non-computation state. Also, Fig. 2.6 shows the two basic braiding operations σ_1 and σ_2. The matrix for the braiding operations σ_1, σ_2 are given by

$$\rho(\sigma_1) = \begin{pmatrix} e^{-i\frac{4}{5}\pi} & 0 & 0 \\ 0 & -e^{-i\frac{2}{5}\pi} & 0 \\ 0 & 0 & -e^{-i\frac{2}{5}\pi} \end{pmatrix}, \tag{2.22}$$

$$\rho(\sigma_2) = \begin{pmatrix} e^{-i\frac{\pi}{5}}\phi^{-1} & -ie^{-i\frac{\pi}{10}}\phi^{-1/2} & 0 \\ -ie^{-i\frac{\pi}{10}}\phi^{-1/2} & -\phi^{-1} & 0 \\ 0 & 0 & -e^{-i\frac{2}{5}\pi} \end{pmatrix}. \tag{2.23}$$

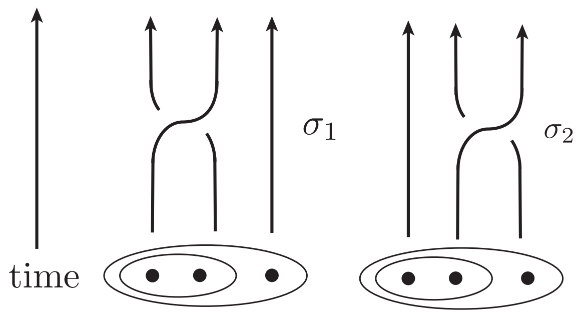

Figure 2.6: Schematic of the braiding operations σ_1, σ_2

Any braiding processes of Fibonacci anyons are built from the elementary braiding σ_1, σ_2, and then the unitary operations are achieved by the combination of $\rho(\sigma_1)$ and $\rho(\sigma_2)$.

Fibonacci anyons can be described by Z_3 parafermion theory, and Z_3 parafermion is realized with a coset model $SU(2)_3/U(1)$ that is equiverent to $SU(2)_3$ Wess-Zumino-Witten model [78, 79]. Z_3 parafermion implies that fermions ψ in this theory satisfy $\psi \times \psi \times \psi = 1$. Thus, Z_k parafermion means that fermions ψ fuse together to the trivial vacuum state if the number of fermions is a multiple of k. In Z_3 parafermion theory, there are six particles $\mathbb{I}, \psi_1, \psi_2, \sigma_1, \sigma_2, \epsilon$. The particle ϵ is the non-Abelian anyon and then is emerged from fusing σ_1 with ψ_1. Of course, this anynon ϵ satisfies the Fibonacci fusion rule $\epsilon \times \epsilon = \mathbb{I} + \epsilon$. This system physically can be realized as $\nu = 12/5$ FQHE state [42, 80].

2.2.3 Yang-Lee Anyons

There is a close cousin of Fibonacci anyon realizable in a non-Hermitian quantum system, which is referred to as Yang-Lee anyons [53, 54]. Yang-Lee anyons obey the same fusion algebra as Fibonacci anyons, which suggests that they may have computational power comparable to Fibonacci anyons. However, Yang-Lee anyons obey *non-unitary non-Abelian statistics*; i.e. the non-Abelian braidings of Yang-Lee anyon are non-unitary because of the non-unitary character of the underlying Conformal Field Theory. Although this feature is not suitable for the application of unitary quantum computation, it may be utilized for the construction of non-unitary quantum gates. Non-unitary quantum computation has been studied in connection with the measurement-based quantum computation [81, 82, 83, 84]. The systematic realization of non-unitary quantum gates may be useful for simulating the non-unitary time-evolution of open quantum systems in a controllable way.

The F-symbol for Yang-Lee anyons can be derived from that for Fibonacci anyons by changing $\phi \to -1/\phi$ with $\phi = (1+\sqrt{5})/2$, which corresponds to the Galois conjugation [53, 54],

$$F = \begin{pmatrix} -\phi & i\sqrt{\phi} \\ i\sqrt{\phi} & \phi \end{pmatrix}. \tag{2.24}$$

Here, the F-symbol acts on the two-dimensional space spanned by the trivial vacuum state and the non-trivial state with a Yang-Lee anyon τ. Note that Eq. (2.24) is a non-unitary matrix, in accordance with the non-unitary CFT for the Yang-Lee edge singularity, in contrast to Fibonacci anyons for which the F-symbol is unitary.

We, here, conjecture that the topological spin of the Yang-Lee anyons is equal to the conformal spin of the non-trivial chiral primary field $h_{1,2} = -1/5$. Then, the R-matrix for Yang-Lee anyons is given by,

$$R^{\tau\tau} = \begin{pmatrix} e^{i\frac{2}{5}\pi} & 0 \\ 0 & e^{i\frac{\pi}{5}} \end{pmatrix}. \tag{2.25}$$

Eqs. (2.24) and (2.25) are the bases for the braiding rule, i.e. the non-Abelian statistics of Yang-Lee anyons. Following the case of Fibonacci anyons [10, 41, 51], we consider the three state $|0\rangle$, $|1\rangle$, and $|N\rangle$ depicted in Fig. 2.5. The matrix for the braiding operations σ_1, σ_2 are given by

$$\rho(\sigma_1) = \begin{pmatrix} e^{i\frac{2}{5}\pi} & 0 & 0 \\ 0 & e^{i\frac{\pi}{5}} & 0 \\ 0 & 0 & e^{i\frac{\pi}{5}} \end{pmatrix}, \tag{2.26}$$

$$\rho(\sigma_2) = \begin{pmatrix} \phi e^{i\frac{3}{5}\pi} & i\sqrt{\phi}e^{-i\frac{\pi}{5}} & 0 \\ i\sqrt{\phi}e^{-i\frac{\pi}{5}} & \phi & 0 \\ 0 & 0 & e^{i\frac{\pi}{5}} \end{pmatrix}. \tag{2.27}$$

Any braiding processes of Yang-Lee anyons are achieved by the combination of $\rho(\sigma_1)$ and $\rho(\sigma_2)$. It is noted that $\rho(\sigma_2)$ is *non-unitary*. Thus, non-Abelian braidings of Yang-Lee anyons give rise to non-unitary transformations on the qubit states. This property can be utilized for the construction of non-unitary quantum circuits [81, 82, 83, 84], which may be useful for simulating dissipative quantum dynamics in a controllable way.

Chapter 3

Introduction to Conformal Field Theory

In this chapter, we briefly introduce Conformal Field Theory (CFT)[85]. [1] This theory is extremely successful for critical phenomena in two dimensions and gives us remarkable results [88, 89, 90]. Generally, the renormalization group method is a powerful tool to access the critical phenomenon and gives us a description to understand the universality of a quantum many-body system [91], but this method does not say what physics on the fixed point follows. It leads to the construction of a theory that rigorously describes the physics on the critical point. The Zamolodchikov c-theorem is a famous example that characterizes critical phenomenon in two dimensions [92]. This theorem says that at a fixed point, a physical value is equal to the central charge c of the CFT. Thus, the CFT can describe the physics at a critical point.

In the previous chapter, we discussed the basic nature of anyons. Anyons physically can be realized as fractionalized quasiparticles in two-dimensional topological phases. In general, low-energy effective field theories of topological phases can be described by $2+1$ Topological Quantum Field Theory (TQFT), Chern-Simons gauge theory [93]. On the other hand, edge states of these systems can be described by $1+1$ CFT, Wess-Zumino-Witten model [4, 42]. Thus, the CFT can identify systems with anyons.

3.1 Conformal Invariance and Virasoro Algebra

[1] We recommend Ref.[86, 87] as a modern textbook to explain CFT.

3.1.1 Conformal transformation in D dimensions

We would like to discuss the general ideas of conformal transformation in a field theory. Let us consider a local field theory in $D(= d+1)$ dimensional spacetime. For $d = 3$, the flat metric tensor $g_{\mu\nu}$ is given by

$$g_{\mu\nu} = \eta_{\mu\nu} = \begin{pmatrix} -1 & 0 & 0 & 0 \\ 0 & 1 & 0 & 0 \\ 0 & 0 & 1 & 0 \\ 0 & 0 & 0 & 1 \end{pmatrix}, \tag{3.1}$$

then the line element ds^2 introduces as follows

$$ds^2 = \sum_{\mu,\nu=0}^{d} g_{\mu\nu} dx^\mu dx^\nu, \tag{3.2}$$

where $\mu = 0, 1, 2, 3$ are the time and space componets and x^μ stands for the 4-vector $x^\mu = (ct, \boldsymbol{x})$. Throughout the rest of this thesis, we will use Einstein's convention. Thus, we can rewrite Eq.(3.2) as

$$ds^2 = g_{\mu\nu} dx^\mu dx^\nu. \tag{3.3}$$

Under a change of coordinates $x^\mu \to x'^\mu$, the change of the metric tensor is

$$g_{\mu\nu} \to g'_{\mu\nu}(x') = \frac{\partial x^\alpha}{\partial x'^\mu} \frac{\partial x^\beta}{\partial x'^\nu} g_{\alpha\beta}(x). \tag{3.4}$$

First, we consider that the metric tensor does not change under a change of coordinates. Under an infinitesimal transformation, $x^\mu \to x'^\mu = x^\mu - \epsilon^\mu$, the metric tensor transforms as

$$g_{\mu\nu} \to g'_{\mu\nu} = g_{\mu\nu} + \partial_\mu \epsilon_\nu + \partial_\nu \epsilon_\mu. \tag{3.5}$$

From the constraint, $g'_{\mu\nu} = g_{\mu\nu}$, we require that

$$\partial_\mu \epsilon_\nu + \partial_\nu \epsilon_\mu = 0. \tag{3.6}$$

Furthermore, acting ∂_ρ on Eq. (3.6), we obtain the important condition $\partial_\mu \partial_\nu \epsilon_\rho = 0$, which implies that ϵ_μ is given by a form $\epsilon_\mu = a_\mu + b_{\mu\nu} x^\nu$, where the tensor $b_{\mu\nu}$ is an anti-symmetric tensor: $b_{\mu\nu} = -b_{\nu\mu}$. The form of ϵ implies that the first term a_μ corresponds to the translational transformation and the second term $b_{\mu\nu} x^\nu$ does to the rotational transformation. Here, we consider an infinitesimal transformation of a scalar field $\phi(x)$. Under this transformation, a scalar field $\phi(x)$ change as

$$\phi(x) \to \phi'(x) = \phi(x) + \epsilon^\alpha G_\alpha \phi(x), \tag{3.7}$$

where we introduce a generator G_a which transforms $\phi(x)$ to other fields. Also, a scalar field satisfies $\phi'(x') = \phi(x)$, which gives a transformational form at x-coordinates as

$$\begin{aligned}\phi(x) \to \phi'(x) &= \phi'(x' + \epsilon) = \phi(x + \epsilon) \\ &= \phi(x) + \epsilon^\alpha \partial_\alpha \phi(x).\end{aligned} \tag{3.8}$$

Therefore, we get the translational and rotational generators as follows,

$$P_\mu = -i\partial_\mu, \qquad L_{\mu\nu} = i(x_\mu \partial_\nu - x_\nu \partial_\mu). \tag{3.9}$$

Also, this transformation is called the *Poincaré* transformation.

Next, we introduce the conformal transformation, which leaves the metric tensor up to a local scale change as,

$$g_{\mu\nu}(x) \to g'_{\mu\nu}(x') = \Lambda(x) g_{\mu\nu}(x). \tag{3.10}$$

Obviously, if the scale factor is $\Lambda(x) = 1$, the consequences bring us back to the above discussion. Let us consider that the scale factor Λ depends on x. Here, we introduce two vector fields V^1_μ, V^2_μ. Under the conformal transformation, the magnitude and angle of these vector fields change. The angle

$$\frac{g_{\mu\nu} V^{1\mu} V^{2\nu}}{\sqrt{|V^1|^2 |V^2|^2}}, \tag{3.11}$$

defined by these vector fields, is invariant under the conformal transformation (an example case is shown in Fig.3.1). We consider the change of the metric tensor under an infinitesimal transformation. For the conformal transformation, we require that,

$$\partial_\mu \epsilon_\nu + \partial_\nu \epsilon_\mu = f(x) \eta_{\mu\nu}, \tag{3.12}$$

where $f(x) = (2/D)\partial_\mu \epsilon^\mu$. Eq. (3.12) gives us the partial differential equation

$$\left(\eta_{\mu\nu} \partial^\rho \partial_\rho + (D-2)\partial_\mu \partial_\nu\right) f(x) = 0. \tag{3.13}$$

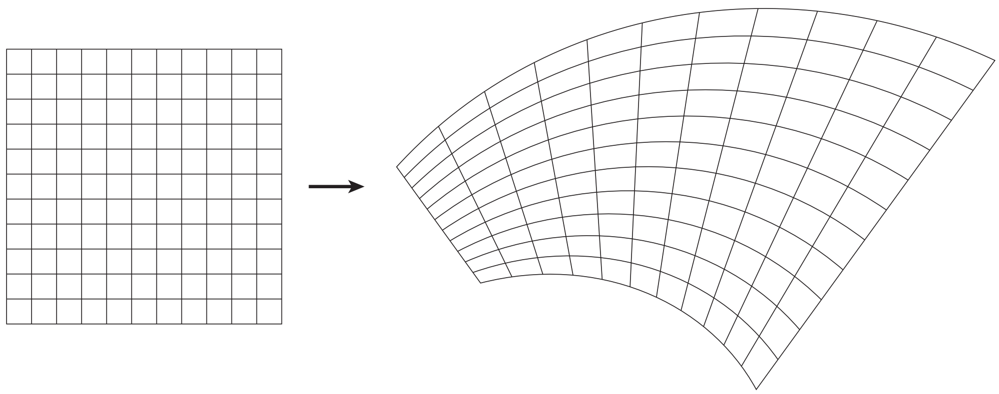

Figure 3.1: Schematic of conformal transformation. A local angle is invariant under conformal transformation.

The solution of this partial differential equation is $f(x) = \alpha + \beta_\mu x^\mu$, which implies

$$\epsilon_\mu = a_\mu + b_{\mu\nu}x^\nu + c_{\mu\nu\rho}x^\nu x^\rho, \tag{3.14}$$

where the tensor $c_{\mu\nu\rho}$ satisfies $c_{\mu\nu\rho} = c_{\mu\rho\nu}$. The conformal transformation contains the translational and the rotational transformation. Obviously, the first term of ϵ corresponds to the translational transformation. For the second term of ϵ, Eq. (3.12) imposes

$$b_{\mu\nu} + b_{\nu\mu} = \frac{2}{D}b^\rho{}_\rho \eta_{\mu\nu}. \tag{3.15}$$

Let us consider the symmetric and anti-symmetric parts of the tensor $b_{\mu\nu}$. The anti-symmetric part of $b_{\mu\nu}x^\nu$ corresponds to the rotational transformation, and the symmetric part $b^\rho{}_\rho x_\mu$ does to the scale transformation because the symmetric part is proportional to the metric tensor $\eta_{\mu\nu}$. For the third term of ϵ, Eq. (3.12) imposes

$$c_{\mu\nu\rho} = -\frac{1}{D}c^\sigma{}_{\sigma\mu}\eta_{\nu\rho} + \frac{1}{D}c^\sigma{}_{\sigma\nu}\eta_{\rho\mu} + \frac{1}{D}c^\sigma{}_{\sigma\rho}\eta_{\mu\nu}. \tag{3.16}$$

The third term $c_{\mu\nu\rho}x^\nu x^\rho$ is called the *special conformal* transformation. Under the special conformal transformation, the position x^μ change as

$$x^\mu \to x'^\mu = x^\mu - \frac{2}{D}(x^\nu c^\sigma{}_{\sigma\nu})x^\mu + \frac{1}{D}|x|^2 c^\sigma{}_{\sigma\mu}. \tag{3.17}$$

Therefore, the conformal transformation consists of the translational, rotational, scale, and special conformal transformation The generators of scale and special conformal transformation can define as,

$$D = -ix^\mu \partial_\mu, \qquad K_\mu = -i(2x_\mu x^\nu \partial_\nu - |x|^2 \partial_\mu). \tag{3.18}$$

For a finite transformation, the conformal transformation is given by

$$x'^\mu = x^\mu - a^\mu, \tag{3.19}$$
$$x'^\mu = \Lambda^\mu{}_\nu x^\nu, \tag{3.20}$$
$$x'^\mu = \lambda x^\mu, \tag{3.21}$$
$$x'^\mu = \frac{x^\mu + B^\mu |x|^2}{1 + 2B^\nu x_\nu + |B|^2 |x|^2}. \tag{3.22}$$

In particular, since we focus on 1+1 dimensional systems, we restrict our discussion to two-dimensional CFT.

3.1.2 Two dimensional CFT

For the discussion on the two-dimensional case, it is useful to replace the real coordinates (x^0, x^1) with a complex variable z and its conjugate $\overline{z}$ as

$$z = x^0 + ix^1, \qquad \overline{z} = x^0 - ix^1. \tag{3.23}$$

From Eq. (3.12), we cloud easily find that $\epsilon(\overline{\epsilon})$ only depends on the complex variable $z(\overline{z})$. Let us consider the conformal transformation $z \to z' = z - \epsilon(z), \overline{z} \to \overline{z}' = \overline{z} - \overline{\epsilon}(\overline{z})$, and then expand $\epsilon(z), \overline{\epsilon}(\overline{z})$ with the form of Laurant series,

$$\epsilon(z) = -\sum_{n=-\infty}^{\infty} \epsilon_n z^{n+1}, \qquad \overline{\epsilon}(\overline{z}) = -\sum_{n=-\infty}^{\infty} \overline{\epsilon}_n \overline{z}^{n+1}. \tag{3.24}$$

The generators of $\epsilon(z)$ and $\overline{\epsilon}(\overline{z})$ can be defined as,

$$l_n = -z^{n+1}\partial = -z^{n+1}\frac{\partial}{\partial z}, \qquad \bar{l}_n = -\overline{z}^{n+1}\overline{\partial} = -\overline{z}^{n+1}\frac{\partial}{\partial \overline{z}}. \tag{3.25}$$

These generators obey this algebra,

$$[l_n, l_m] = (n-m)l_{n+m}, \qquad [\bar{l}_n, \bar{l}_m] = (n-m)\bar{l}_{n+m}. \tag{3.26}$$

Eq. (3.25) implies that the two-dimensional conformal transformation consists of infinite generators. [2] The case of $n = -1, 0, 1$ is globally defined in the Riemann sphere, which implies that these generators correspond to the generators of the conformal transformation

$$\begin{aligned}
&P_\mu : l_{-1} = -\partial, \bar{l}_{-1} = -\overline{\partial}, \\
&L_{\mu\nu} : i(l_0 - \bar{l}_0) = -i(z\partial - \overline{z}\overline{\partial}), \\
&D : l_0 + \bar{l}_0 = -z\partial - \overline{z}\overline{\partial}, \\
&K_\mu : l_1 = -z^2\partial, \bar{l}_1 = -\overline{z}^2\overline{\partial}.
\end{aligned}$$

The algebra composed of the above generators is called the *global conformal algebra*.

An elementary field in CFT is the primary field $\phi(z,\overline{z})$ which transforms as,

$$\phi(z,\overline{z}) \to \phi'(z',\overline{z}') = \left(\frac{dz}{dz'}\right)^h \left(\frac{d\overline{z}}{d\overline{z}'}\right)^{\overline{h}} \phi(z,\overline{z}), \tag{3.27}$$

under an arbitrary transformation $(z,\overline{z}) \to (z',\overline{z}')$. This parameters $(h,\overline{h})$ are called *conformal weight*. Also, we can define the quasi primary field which transforms as, Eq. (3.27) under the global conformal transformation. [3] Under the infinitesimal transformation, $z \to z' = z - \epsilon(z)$, a primary field $\mathcal{O}(z,\overline{z})$ changes as

$$\mathcal{O}(z,\overline{z}) \to \mathcal{O}'(z,\overline{z}) = \mathcal{O}(z,\overline{z}) + \left[h\left(\partial\epsilon(z)\right) + \epsilon(z)\partial + \overline{h}\left(\overline{\partial}\overline{\epsilon}(\overline{z})\right) + \overline{\epsilon}(\overline{z})\overline{\partial}\right]\mathcal{O}(z,\overline{z}). \tag{3.28}$$

This consequence can be regarded as the definition of a primary field $\mathcal{O}(z,\overline{z})$.

One of the most valuable features of two-dimensional CFT is that holomorphic and anti-holomorphic parts always are independent. Furthermore, the global conformal transformation uniquely gives the coordinate dependence of a two point correlation function as

$$\langle\phi_1(z,\overline{z})\phi_2(w,\overline{w})\rangle = \frac{\delta_{h_1,h_2}\delta_{\overline{h}_1,\overline{h}_2}}{|z-w|^{2h_1}|\overline{z}-\overline{w}|^{2\overline{h}_1}}. \tag{3.29}$$

Next, we would like to discuss the role of the energy-momentum tensor $T^\mu{}_\nu$ in CFT. The energy-momentum tensor is closely related to the symmetry and the

[2] In $D(>2)$ dimensions, the conformal transformation consists of finite generators $P_\mu, L_{\mu\nu}, D, K_\mu$.

[3] In CFT, there are some fields that are quasi primary fields but not primary fields. For example, an energy-momentum tensor $T^\mu{}_\nu$ is one of quasi primary fields.

conserved quantity of a system. [4] In field theories, the energy-momentum tensor $T^{\mu}{}_{\nu}$ can be defined as an invariant current under the translational transformation. [5] Let us consider the action,

$$S = \int dt L = \int d^d x \mathcal{L}(\phi, \partial_\mu \phi), \tag{3.31}$$

where $\mathcal{L}$ is the lagrangian density of a system. For this case, the energy-momentum tensor can be defined as,

$$T^{\mu}{}_{\nu} = \frac{\partial \mathcal{L}}{\partial(\partial_\mu \phi)} \partial_\nu \phi - \delta^{\mu}{}_{\nu} \mathcal{L}, \tag{3.32}$$

where we can write the current j^μ under the scale transformation as $T^{\mu}{}_{\nu} x^\nu$. The invariant of this current j^μ implies that the energy-momentum tensor $T^{\mu}{}_{\nu}$ must be traceless $T^{\mu}{}_{\mu} = 0$. Through the rest discussion, we replace $T^{\mu}{}_{\nu}$ with

$$T \equiv -2\pi T_{zz}, \qquad \overline{T} = -2\pi T_{\overline{z}\overline{z}}. \tag{3.33}$$

From the Ward-Takahashi identity, we get the correlation functions with the energy-momentum tensor satisfying,

$$\langle T(z) O_1 \cdots O_n \rangle = \sum_{j=1}^{n} \left(\frac{1}{z - z_j} \frac{\partial}{\partial z_j} + \frac{h_j}{(z - z_j)^2} \right) \langle O_1 \cdots O_n \rangle + \ldots, \tag{3.34}$$

$$\left\langle \overline{T}(\overline{z}) O_1 \cdots O_n \right\rangle = \sum_{j=1}^{n} \left(\frac{1}{\overline{z} - \overline{z}_j} \frac{\partial}{\partial \overline{z}_j} + \frac{\overline{h}_j}{(\overline{z} - \overline{z}_j)^2} \right) \langle O_1 \cdots O_n \rangle + \ldots, \tag{3.35}$$

where O_n is primary fields and $\ldots$ is the holomorphic function that has no divergence at $z = z_j (\overline{z} = \overline{z}_j)$. This equation implies that the energy-momentum tensor $T^{\mu}{}_{\nu}$ is the quasi primary field with the conformal weight $(h, \overline{h}) = (2, 0)$.

[4] In quantum field theories, Ward-Takahashi identity is an important identity for the discussion on the symmetry of a system [94, 95]. This identity implies that a current is invariant at the position without a field $\phi(x)$.

[5] For an arbitrary transformation, the current is defined as,

$$j^{\mu}{}_{a}(x) = \frac{\partial \mathcal{L}}{\partial(\partial_\mu \phi)} G_a \phi - \mathcal{J}^{\mu}{}_{a}, \tag{3.30}$$

which satisfies $\partial_\mu j^{\mu}{}_{a}(x) = 0$ and that the action S is invariant up to the surface term $\epsilon^a \partial_\mu \mathcal{J}^{\mu}{}_{a}$. The current $j^{\mu}{}_{a}$ is called the Noether currents [96].

Now, we introduce the operator product expansion (OPE) that a product of two fields can be expanded as

$$\mathcal{O}_1\mathcal{O}_2 = \sum_p C^p_{12}(z,w)\mathcal{O}_p(w), \tag{3.36}$$

where fields $\mathcal{O}_p$ form a complete system. The OPE of $T(z)T(w)$ is

$$T(z)T(w) \sim \frac{c/2}{(z-w)^4} + \frac{2T(w)}{(z-w)^2} + \frac{\partial T(w)}{z-w}, \tag{3.37}$$

where c is called *central charge* and a number that reflects the universality class of the CFT. In unitary field theories, this charge is a non-negative value. Also, the central charge c shows the number of degrees of freedom in a system. For example, this charge c of N free boson systems is equal to N, and that of N free fermion systems is $N/2$. Under an infinitesimal transformation ,$z \to z' = z - \epsilon(z)$, the energy-momentum tensor $T(z)$ changes as

$$T(z) \to T'(z) = T(z) + (2\partial\epsilon(z) + \epsilon(z)\partial)T(z) + \frac{c}{12}(\partial^3\epsilon(z))T(z). \tag{3.38}$$

Also, under a finite transformation, the energy-momentum tensor changes as

$$T'(z') = \left(\frac{dz}{dz'}\right)^2 \left(T(z) - \frac{c}{12}\{z';z\}\right), \tag{3.39}$$

where the symbol $\{;\}$ is called *Schwarzian derivative* and is defined as

$$\{z';z\} \equiv \frac{\partial^3 z'(z)}{\partial z'(z)} - \frac{3}{2}\left(\frac{\partial^2 z'(z)}{\partial z'(z)}\right)^2. \tag{3.40}$$

For the anti-holomorphic part $\overline{T}(\overline{z})$, the above equations only require replacing $c \to \overline{c}$. In general, the central charge c and $\overline{c}$ could be different, then CFT is chiral. The modular invariance imposes that the two central charges $c, \overline{c}$ must be equal [97]. [6] This invariance is usually required. Chiral systems are the edge states of the

[6]The partition function Z, as a function of τ, of a system is invariant under the following transformation:

$$\tau \to \frac{1}{\tau}, \qquad \tau \to \tau + 1, \tag{3.41}$$

which implies that this system possesses modular symmetry.

fractional quantum Hall system, topological superconductor, topological superfluid, and so on. Also, the central charge is an example of a *quantum anomaly*. Quantum anomaly is an additional term that is induced by a coordinate transformation or gauge transformation. This anomaly implies that a symmetry that survives in the classical theories is broken due to a quantum anomaly in the quantum theories. In classical field theories, the central charge c is absent, which means that the energy-momentum tensor $T(z)$ homogeneous transforms under a finite transformation. Thus, the central charge c, *confromal anomaly*, is a quantum effect that breaks the homogeneous transformation.

Physical Meaning of the Centaral Charge c

The central charge means the quantum effect that smoothly violates the conformal symmetry. Also, the central charge c plays a crucial role as the universal finite-size correction of the ground state energy E_{gs} [88, 89]. Let us consider the conformal transformation, $z \to w = u + iv = \frac{l}{2\pi} \ln z$, which is a mapping from the infinite flat plane to the cylinder. In this case, the energy-momentum tensor, $T_{uu} = T(v) + \overline{T}(v)$, means the density of the energy flow. From the Schwarzian derivative, the energy-momentum tensor T yields the following equation

$$T(w) = \left(\frac{2\pi}{l}\right)^2 \left(z^2 T(z) - \frac{c}{24}\right). \tag{3.42}$$

Thus, the Hamiltonian is given by

$$H = \frac{1}{2\pi} \int_0^l \left[T(v) + \overline{T}(v)\right] dz = \frac{2\pi}{l}(L_0 + \overline{L}_0) - \frac{\pi c}{6l}. \tag{3.43}$$

This result implies that the ground state energy E_{gs} is $-\frac{\pi c}{6l}$, where the ground state is defined as $L_0 |0\rangle = \overline{L}_0 |0\rangle = 0$.

3.1.3 Virasoro Algebra and Hilbert Space

Let us consider the Hilbert space in two-dimensional CFTs. We would like to switch from the path integral formalism to the operator formalism to discuss the Hilbert space. In the path integral formalism, the order of fields ϕ does not have any meaning, while in the operator formalism, the order is not negligible. We adopt the radial quantization with time. This quantization is the method that maps from the cylinder to the complex plane in Fig. 3.2. The relation between the cylinder and the

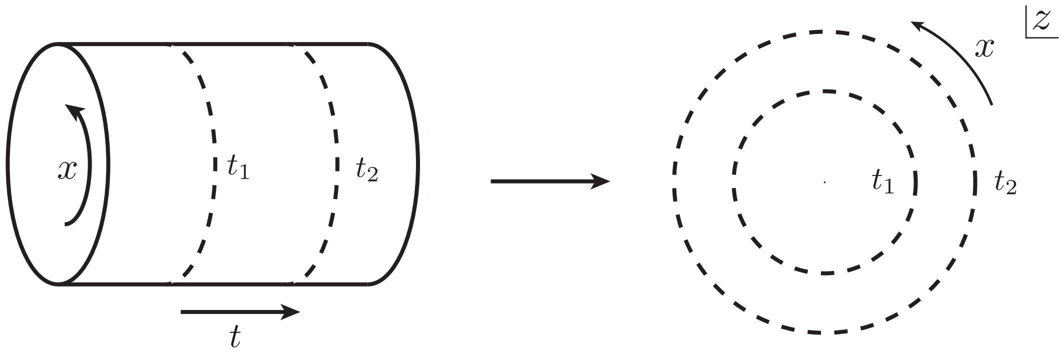

Figure 3.2: Schematic of mapping from the cylinder to the complex plane

complex plane is given by

$$z \equiv \exp(t + ix), \qquad \overline{z} \equiv \exp(t - ix). \tag{3.44}$$

In the operator formalism, the initial state is the state at $z = 0(t \to -\infty)$, and then the final state is the state at $z \to \infty(t \to \infty)$. Now we define the initial state $|\mathcal{O}\rangle$ with a field $\mathcal{O}(z, \overline{z})$ acting on the vacuum state as,

$$|\mathcal{O}\rangle = \lim_{z,\overline{z}\to 0} \mathcal{O}(z, \overline{z}) |0\rangle \,, \tag{3.45}$$

where the vacuum state $|0\rangle$ means the state that expresses the absence of a field at $z = 0$. Similarly, we can define the final state $\langle\mathcal{O}|$ with acting a field $\mathcal{O}$ on the vacuum state as,

$$\langle\mathcal{O}| = \lim_{z,\overline{z}\to \infty} \overline{z}^{2h} z^{2\overline{h}} \langle 0| \mathcal{O}(\overline{z}, z), \tag{3.46}$$

where we switch the coordinates $z \to w = 1/\overline{z}$. [7] Since we can define the final state as the hermitian conjugate of the initial state, the hermitian conjugate of a field $\mathcal{O}(z, \overline{z})$ can be introduced as

$$(\mathcal{O}(z, \overline{z}))^\dagger = \overline{z}^{-2h} z^{-2\overline{h}} \mathcal{O}(1/\overline{z}, 1/z). \tag{3.48}$$

[7] We need to map the coordinates where the state with $t \to \infty$ corresponds to the state at $w = 0$. Under this transformation $w \to z$, a field $\mathcal{O}'(w, \overline{w})$ transforms as,

$$\mathcal{O}'(w, \overline{w}) = \left(\frac{d\overline{z}}{dw}\right)^h \left(\frac{dz}{d\overline{w}}\right)^{\overline{h}} \mathcal{O}(z, \overline{z}) = (-1)^{h+\overline{h}} \overline{z}^{2h} z^{2\overline{h}} \mathcal{O}(z, \overline{z}). \tag{3.47}$$

Generally, a primary (quasi-primary) field $\phi(z, \overline{z})$ with the conformal weight $(h, \overline{h})$ can be expressed as,

$$\phi(z, \overline{z}) = \sum_{n,m=-\infty}^{\infty} z^{-m-h} \overline{z}^{-n-\overline{h}} \phi_{n,m}, \tag{3.49}$$

$$\phi_{n,m} = \frac{1}{2\pi i} \oint dz z^{n+h-1} \frac{1}{2\pi i} \oint d\overline{z} \overline{z}^{m+\overline{h}-1} \phi(z, \overline{z}), \tag{3.50}$$

using a mode expansion. The Noether current under the conformal transformation is related to the energy-momentum tensor $T^{\mu}{}_{\nu}$, which implies that the mode operators for the energy-momentum tensor $T^{\mu}{}_{\nu}$ are the generators of the conformal transformation on the Hilbert space in two-dimensional CFT. The generators $l_n, \bar{l}_n$ (Eq.(3.25)) are the generators of the conformal transformation on the spacetime. We expand the energy-momentum tensor $T^{\mu}{}_{\nu}$ based on Eq.(3.50) as follows

$$T(z) = \sum_{n=-\infty}^{\infty} z^{-n-2} L_n, \qquad \overline{T}(\overline{z}) = \sum_{n=-\infty}^{\infty} \overline{z}^{-n-2} \overline{L}_n, \tag{3.51}$$

$$L_n = \frac{1}{2\pi i} \oint dz z^{n+1} T(z), \qquad \overline{L}_n = \frac{1}{2\pi i} \oint d\overline{z} \overline{z}^{n+1} \overline{T}(\overline{z}). \tag{3.52}$$

The generators $L_n, \overline{L}_n$ satisfy the following commutation relation:

$$[L_n, L_m] = (n-m) L_{n+m} + \frac{c}{12} n(n^2-1) \delta_{n+m,0}, \tag{3.53}$$

$$[\overline{L}_n, \overline{L}_m] = (n-m) \overline{L}_{n+m} + \frac{c}{12} n(n^2-1) \delta_{n+m,0}, \tag{3.54}$$

$$[L_n, \overline{L}_m] = 0. \tag{3.55}$$

and is called the *Virasoro generator*, then this algebra is called the *Virasoro algebra*. [8] For $n = -1, 0, 1$, Virasoro algebra corresponds to the global conformal algebra. Furthermore, the generator of the scale transformation $L_0 + \overline{L}_0$ means the Hamiltonian in the radial quantization, which implies that the analysis of spectra in a system is equal to that of conformal weights. The global conformal algebra would satisfy the following algebra

$$[l_n, l_m] = (n-m) l_{m+n}. \tag{3.56}$$

We would like to add a central extension term to this algebra. In mathematics, this procedure is called *Lie algebra extension*. *Central* means that this term always

[8] From the Ward-Takahashi identity and the OPE, we can obtain the Virasoro algebra.

commutes with all operators. In general, the Lie algebra extension of this algebra can be given by

$$[L_n, L_m] = (n-m)L_{m+n} + c_{n,m}, \tag{3.57}$$

where $c_{n,m}$ is center and satisfies $c_{n,m} = -c_{m,n}$. On the global conformal algebra, a non-trivial central extension term is only $\frac{c}{12}n(n^2-1)\delta_{n+m,0}$. [9] Thus, the Virasoro algebra is unique to the Lie algebra extension of the global conformal algebra.

The energy-momentum tensor $T(z)$ is well-defined in the Riemann sphere, which implies that there is no singularity at $z = 0$. This consequence imposes an important constraint as

$$L_n |0\rangle = 0 \qquad n \geq -1, \tag{3.59}$$
$$\langle 0| L_n = 0 \qquad n \leq 1. \tag{3.60}$$

Also, the Virasoro generators $L_n^\dagger$ satisfy $L_n^\dagger = L_{-n}$. Therefore, the vacuum state is invariant under the global conformal transformation:

$$L_n |0\rangle = \langle 0| L_n = 0 \ (n = 0, \pm 1). \tag{3.61}$$

Conformal Tower

The initial state with a primary field $\mathcal{O}(z, \overline{z})$ acting on the vacuum state is

$$\left|h, \overline{h}\right\rangle = \lim_{z,\overline{z}\to 0} \mathcal{O}(z, \overline{z}) |0\rangle, \tag{3.62}$$

where the conformal weight of the primary field $\mathcal{O}(z, \overline{z})$ is $(h, \overline{h})$. This initial state is called a *primary state*. The primary state is the eigenstate of the operator $L_0, \overline{L}_0$:

$$L_n \left|h, \overline{h}\right\rangle = \begin{cases} 0 & n > 0 \\ h \left|h, \overline{h}\right\rangle & n = 0 \end{cases}, \overline{L}_n \left|h, \overline{h}\right\rangle = \begin{cases} 0 & n > 0 \\ \overline{h} \left|h, \overline{h}\right\rangle & n = 0 \end{cases}. \tag{3.63}$$

[9] From the Jacobi identity, we obtain

$$(n-m)c_{l,n+m} + (m-l)c_{n,m+l} + (l-n)c_{m,l+n} = 0. \tag{3.58}$$

For the replacement of the operator, $L_n \to L_n + c_n$, $c_{n,m} \to c_{n,m} - (n-m)c_{n+m}$, $\frac{c}{12}n(n^2-1)\delta_{n+m,0}$ is only non-vanishing term.

[10] These conditions can be regarded as the definition of the primary state and are called *Primary* conditions. For the final state, we can define the primary state as,

$$\langle h,\overline{h}| = \lim_{z,\overline{z}\to\infty} z^{2\overline{h}}\overline{z}^{2h}\langle 0|\mathcal{O}(z,\overline{z}), \tag{3.65}$$

while the primary conditions are,

$$\langle h,\overline{h}| L_{-n} = \begin{cases} 0 & n>0 \\ h\langle h,\overline{h}| & n=0 \end{cases}, \langle h,\overline{h}| \overline{L}_{-n} = \begin{cases} 0 & n>0 \\ \overline{h}\langle h,\overline{h}| & n=0 \end{cases}. \tag{3.66}$$

Let us discuss how to introduce general states by the primary state. The basic idea of constructing general states is the same as for the angular momentum case. In the angular momentum case, the eigenstates satisfy the following condition,

$$J^3|j,m\rangle = m|j,m\rangle, \qquad \mathcal{J}|j,m\rangle = j(j+1)|j,m\rangle, \tag{3.67}$$

where $j\geq 0$, the operators J^i satisfy $[J^i,J^j]=i\epsilon_{ijk}J^k$ and the operator $\mathcal{J}$ can be defined as $\mathcal{J}\equiv J^iJ^i$. [11] We can also define the ladder operators as $J^{\pm}\equiv J^1\pm iJ^2$, which implies that states with $J^{\pm}$ acting on the state $|j,m\rangle$ are,

$$J^{\pm}|j,m\rangle \propto |j,m\pm 1\rangle. \tag{3.68}$$

Therefore, acting on the ladder operators $J^{\pm}$ to the states $|j,m\rangle$ can construct the states that the eigenvalue of J^3 only differs by ± 1, but that of $\mathcal{J}$ is the same value. Now, let us focus on the state $|j,j\rangle$. From the features of the ladder operators $J^{\pm}$, we obtain $J^+|j,j\rangle=0$. [12] This consequence implies that acting on J^+ to $|j,j\rangle$ cannot construct other states, while acting on J^- to $|j,j\rangle$ can construct other states as,

$$(J^-)^{j-m}|j,j\rangle \propto |j,m\rangle, \tag{3.69}$$

where j and m satisfy the following inequality: $-j\leq m\leq j$. [13]

[10]From the OPE, we obtain

$$L_n|h,\overline{h}\rangle = \oint \frac{dz}{2\pi i} z^{n+1}T(z)|h,\overline{h}\rangle = \begin{cases} 0 & n>0 \\ h|h,\overline{h}\rangle & n=0 \end{cases} \tag{3.64}$$

, and the anti-holomorphic case shows the same result.

[11]In the Lie algebra, the eigenstates of the angular momentum are the highest weight states of the $\mathfrak{su}_2$ algebra.

[12]From $J^{\mp}J^{\pm}=\mathcal{J}-J^3J^3\mp J^3$, acting on J^-J^+ to $|j,j\rangle$ gives $J^-J^+|j,j\rangle=0$.

[13]We require that squared norms of $J^{\pm}|j,m\rangle$ are non-negative.

We apply the argument above to the primary state. To simplify the later discussion, we would like to focus on the holomorphic part. For the anti-holomorphic part, the same discussion is valid. From the primary condition (3.63), we found that the Virasoro operators $L_n(n>0)$ correspond to the operator J^+, while $L_{-n}(n>0)$ do the operator J^-. Thus, acting on $L_{-n}(n>0)$ to the primary state can construct other states. In general, these states can be given by

$$L_{-n_1}\cdots L_{-n_M}\left|h\right\rangle \qquad 1\le n_1\le\cdots\le n_M. \tag{3.70}$$

These states, of course, are the eigenstate with the eigenvalue $h+N$ of the operator L_0 where $N\equiv\sum_{k=1}^{M}n_k$, and are called *descendant* states. The integer N means the level of the descendant states. The descendant state $L_{-n}\left|\mathcal{O}\right\rangle$ can be regarded as the vacuum state, at $w=0$, with the following field,

$$\mathcal{O}^{-n}(w)=\frac{1}{2\pi i}\oint dz(z-w)^{-n+1}T(z)\mathcal{O}(w). \tag{3.71}$$

This field is called a *descendant field*. [14] Furthermore, we easily obtain the general form of the level N descendant field from the OPE.

The number of the descendant states $p(N)$ analytically are known as,

$$\frac{1}{\prod_{n=1}^{\infty}(1-q^n)}=\sum_{N=1}^{\infty}p(N)q^N=1+q+2q^2+3q^3+\cdots. \tag{3.72}$$

Tab. 3.1 shows examples of the descendant states. This family of the descendant

Level N	descendant state	$p(N)$
0	$\left\|h\right\rangle$	1
1	$L_{-1}\left\|h\right\rangle$	1
2	$L_{-2}\left\|h\right\rangle, L_{-1}L_{-1}\left\|h\right\rangle$	2
3	$L_{-3}\left\|h\right\rangle, L_{-1}L_{-2}\left\|h\right\rangle, L_{-1}L_{-1}L_{-1}\left\|h\right\rangle$	3

Table 3.1: Examples of the descendant states

states is called a *Conformal Family(Tower)* (Fig. 3.3) or *Verma module*. Notably, the conformal family forms a subspace of the Hilbert space. Thus, acting the Virasoro operators, the states of a conformal family can not violate the states of another conformal family.

[14] In particular, the energy-momentum tensor $T(z)$ is the level 2 descendant field for the trivial field $\mathbb{I}$.

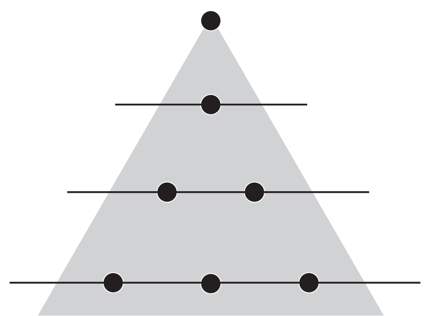

Figure 3.3: Schematic of a Conformal Tower

3.1.4 Minimal Model

Generally, all states of a conformal tower transfer each other, which implies that the representation of the Virasoro algebra is an *irreducible representation*. However, in the model with specific conformal weight, this algebra is *reducible*. This irreducible representation is called a *degenerate representation*. The character of a minimal model is that descendant states could satisfy the primary condition. These states are orthogonal to other states of a minimal model and have zero-norm, and are called a *Singular Vector* or *Null vector*.

For the level 1 descendant states, a singular vector is the vacuum state $|0\rangle$. For the level 2 descendant states, a singular vector would be given by

$$|\chi\rangle = (L_{-2} + aL_{-1}L_{-1})\,|h\rangle\,. \tag{3.73}$$

We should find a conformal weight h and a variable a satisfying the primary condition. The primary condition is $L_n\,|\chi\rangle = 0$ $(n > 0)$, $L_0\,|\chi\rangle = (h+2)\,|\chi\rangle$. From the primary condition, we obtain

$$L_1\,|\chi\rangle = [3 + 2a(2h+1)]\,L_{-1}\,|h\rangle = 0, \tag{3.74}$$

$$L_2\,|\chi\rangle = \left(4h + \frac{c}{2} + 6ha\right)|h\rangle = 0. \tag{3.75}$$

Thus, if

$$a = -\frac{3}{2(2h+1)}, \qquad h = \frac{1}{16}\left(5 - c \pm \sqrt{(1-c)(25-c)}\right), \tag{3.76}$$

the descendant state is a singular vector. At the higher level, we can obtain a singular vector similarly.

We have studied the Hilbert space for CFT, but it is non-trivial whether a conformal family is unitary. Now, unitarity means that the inner product of all states is definitely non-negative. [15] At level 2, there are two descendant states, which implies that we need to check the inner product for all combinations. This problem is equivalent to the determination of the following matrix,

$$
\begin{aligned}
M_2(c,h) &= \begin{pmatrix} \langle h| L_1 L_1 L_{-1} L_{-1} |h\rangle & \langle h| L_1 L_1 L_{-2} |h\rangle \\ \langle h| L_2 L_{-1} L_{-1} |h\rangle & \langle h| L_2 L_{-2} |h\rangle \end{pmatrix} \\
&= \begin{pmatrix} 4h(2h+1) & 6h \\ 6h & 4h + c/2 \end{pmatrix}.
\end{aligned} \tag{3.77}
$$

Since this matrix $M_2(c,h)$ is a hermitian matrix, the unitary condition is that the eigenvalues of $M_2(c,h)$ are non-negative. Thus, the determinant of $M_2(c,h)$ is non-negative. If $\det\{M_2(c,h)\} = 0$, the conformal weights as a function of the central charge are

$$
h(c) = 0, \frac{1}{16}\left(5 - c \pm \sqrt{(1-c)(25-c)}\right). \tag{3.78}
$$

These consequences correspond to the conformal weight of the above singular vectors. Thus, the determinant of the matrix $M_2(c,h)$ sufficiently informs us of unitarity and singular vectors. At level N, the analysis of the determinant of the matrix $M_N(c,h)$ is usually challenging, but Kac gave a rigorous expression for the determinant as,

$$
\det\{M_N(c,h)\} = \alpha_N \prod_{r,s\geq 1, rs\leq N} (h - h_{r,s}(c))^{p(N-rs)}, \tag{3.79}
$$

where α_N is a positive constant [98, 99, 100]. The central charge c and the conformal weight $h_{r,s}(c)$ are given by,

$$
c = 13 - 6\left(\eta + \frac{1}{\eta}\right),\ h_{r,s}(\eta) = \frac{1}{4}\left[(r^2-1)\eta + (s^2-1)\frac{1}{\eta}\right] - \frac{1}{2}(rs-1). \tag{3.80}
$$

In particular, for $\eta = q/p (p > q)$ and p, q are prime integers of each other, the central charge c and the conformal weight $h_{r,s}(c)$ become

$$
c = 1 - \frac{6(p-q)^2}{pq},\ h_{r,s} = \frac{(pr-qs)^2 - (p-q)^2}{4pq}, \tag{3.81}
$$

[15] In general, unitarity for CFT requires that the central charge c and the conformal weight h must be positive.

where $1 \leq r < q, 1 \leq s < p$. This model is called a *Minimal Model* $\mathcal{M}_{p,q}$ [85]. Notably, the conformal family of the degenerate representation is closed with respect to the *Fusion Rule*

$$\mathcal{O}_{r_1,s_1} \times \mathcal{O}_{r_2,s_2} = \sum_{\substack{n=1+|r_1-r_2|, \\ n+r_1+r_2=1 \mod 2}}^{r_1+r_2-1} \sum_{\substack{m=1+|s_1-s_2|, \\ m+s_1+s_2=1 \mod 2}}^{s_1+s_2-1} \mathcal{O}_{n,m}, \tag{3.82}$$

where $\mathcal{O}_{r,s}$ is the primary field with the conformal weight $h_{r,s}$. [16] Hereafter, we would like to introduce some examples of the minimal model $\mathcal{M}_{p,q}$.

Ising Model

Let us consider the Ising model on $2D$ lattice without a magnetic field. The Hamiltonian is given by

$$\mathcal{H} = -\frac{J}{2} \sum_{i,j} \sigma_i \sigma_j = -\frac{J}{2} \sum_{i} \epsilon_i, \tag{3.83}$$

where σ_i is the Ising spin variable at site i which can take one of two possible values ± 1 and ϵ_i is the energy density defined as $\epsilon_i \equiv \sum_j \sigma_i \sigma_j$. At the critical point T_c, the two point correlation functions of both $\sigma_i \sigma_j$ and $\epsilon_i \epsilon_j$ is known as

$$\langle \sigma_i \sigma_j \rangle \sim \frac{1}{{r_{i,j}}^{1/4}}, \ \langle \epsilon_i \epsilon_j \rangle \sim \frac{1}{{r_{i,j}}^{2}}, \tag{3.84}$$

where $r_{i,j}$ is the distance between site i and site j [101, 102, 103]. There are two scaling operators σ, ϵ in the critical Ising model. The operator σ means the spin operator that corresponds to a continuum version of the Ising spin variables σ_i, and the operator ϵ means the energy operator that corresponds to a continuum version of the interaction energy variables $\sigma_i \sigma_{i+1}$. Thus, the above two point correlation functions are equal to the two point correlation functions of both $\sigma(z, \overline{z})$ and $\epsilon(z, \overline{z})$. The scaling dimensions of σ, ϵ are $\Delta_\sigma = 1/8, \Delta_\epsilon = 1$.

On the other hand, primary fields of the minimal model $\mathcal{M}_{4,3}$ are

$$\begin{cases} \text{trivial field } \mathbb{I} & h_{1,1} = h_{2,3} = 0, \\ \text{non-trivial field } \sigma & h_{1,2} = h_{2,2} = \frac{1}{16}, \\ \text{non-trivial field } \epsilon & h_{2,1} = h_{1,3} = \frac{1}{2}. \end{cases} \tag{3.85}$$

[16] The fusion rule can be derived from *Belavin-Polyakov-Zamolodchikov* equations for the correlation function of primary fields.

Also, the fusion rule is given by

$$\sigma = \mathbb{I} + \epsilon, \ \sigma = \epsilon, \ \epsilon = \mathbb{I}. \tag{3.86}$$

In CFT, a scaling dimension is defined as $\Delta \equiv h + \overline{h}$. Thus, the scaling dimensions of σ, ϵ are $\Delta_\sigma = 1/8, \Delta_\epsilon = 1$. The minimal model $\mathcal{M}_{4,3}$ describes the critical Ising model on $2D$ lattice. There are other examples of the minimal model $\mathcal{M}_{p,q}$: $\mathcal{M}_{5,4}$ is the tricritical Ising model [104], $\mathcal{M}_{6,5}$ is the three-state Potts model [105], and $\mathcal{M}_{p+1,p} (p \geq 3)$ is the RSOS model [106, 107].

Yang-Lee Singularity

Yang-Lee model $\mathcal{H}_{YL}$ is the transverse 1D Ising model with a pure imaginary magnetic field ih:

$$\mathcal{H}_{\rm YL} = -\sum_{j=1}^{L} \left[J S_j^z S_{j+1}^z + \Gamma S_j^x + ih S_j^z \right], \tag{3.87}$$

where $S_j^{x,y,z}$ is the spin 1/2 operator at site j, and L is the system size. The partition function of this model could be zero on the complex plane of physical parameters. These zeros are called *Yang-Lee zeros*, and could characterize the phase transition [108, 109]. Fig. 3.4 is the schematic of the distribution of the Yang-Lee zeros. The

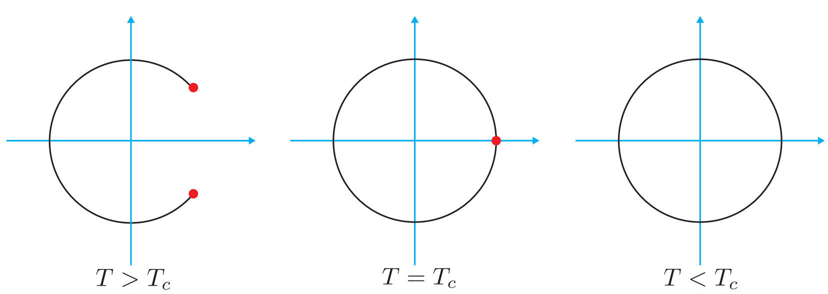

Figure 3.4: Distribution of the zeros of the partition function as a function of temperature T.

magnetization of this model exhibits singular behavior with a negative exponent close to the critical magnetic field h_c and then this *non-unitary* critical behavior is called a *Yang-Lee edge singularity*. From the renormalization group method, the component σ of the magnetization is $-1/6$ in thermodynamic limit [110]. Also, this non-unitary critical phenomenon can be described by the non-unitary CFT [111]. This non-unitarity model is the minimal model $\mathcal{M}_{5,2}$ with the central charge $c = -22/5$ and the conformal weight $h = -1/5$. For $p = 5, q = 2$, there are two primary fields,

$$\begin{cases} \text{trivial field } \mathbb{I} & h_{1,1} = h_{1,4} = 0, \\ \text{non-trivial field } \tau & h_{1,2} = h_{1,3} = -\frac{1}{5}. \end{cases} \tag{3.88}$$

Also, the fusion rule is given by

$$\tau \times \tau = \mathbb{I} + \tau. \tag{3.89}$$

The CFT description of the Yang-Lee edge singularity in the 2D Ising model with an imaginary magnetic field was confirmed by numerical studies [112, 113]. The experimental observation of the Yang-Lee zeros was achieved by measuring the quantum coherence of a probe spin coupled to an Ising spin bath [114, 115].

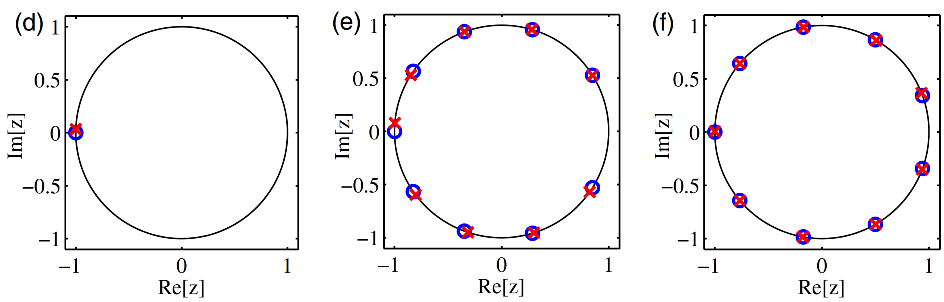

Figure 3.5: Observation of Yang-Lee zeros [115]. The red crosses mean the observation data measured from the zeros of probe spin coherence, and the blue circles mean the theoretical predictions of the Yang-Lee zeros. The temperature of each data is (d)$T = 300K$, (e)$T_{eff} = 15J/8$, and (f)$T_{eff} = 9J/40$, where J is the coupling strength of the bath and the effective temperature T_{eff} is scaled by J.

3.2 Renomalization group and CFT

The traditional studies for the critical phenomenon are based on soluble models [116, 117], scaling hypothesis [118, 119, 120], and the renormalization group(RG) [91]. However, it is worth constructing the theory to explain the physics of critical points. In Sec.3.1, we gave some examples of the minimal model to describe the specific critical phenomenon. Generally, it is non-trivial whether CFT can explain the physics at critical points. In 1986, Zamolodchikov proposed the theorem, referred to as Zamolodchikov c-theorem: a physical quantity, at a fixed point, is equal to the central charge c of the CFT in $2D$ [92].

In this section, we would like to discuss the relationship between RG and CFT. First of all, we briefly introduce the essence of RG for the description of critical phenomena. At critical points, the correlation length ξ of a system diverges, which implies that the system gets an additional symmetry: scale invariance. From the point of view of scale invariance, Zamolodchikov studied the relationship between scale invariance and conformal invariance. His theorem implies that the two-point correlation function of the energy-momentum tensor at a fixed point could be consistent with the result of CFT.

3.2.1 Renomalization Group

At critical points, the correlation length ξ is infinite, and then we must focus on long-distance physics. The key of RG is to analyze the contribution of this system by integrating out the short distance.

In path integral form, we can represent the partition function as

$$Z = \int \mathcal{D}\phi e^{-S[\phi]}, \tag{3.90}$$

where an action S is a function of a filed ϕ. We define the symbol $\int \mathcal{D}_\Lambda \phi$ as integrating up to a specific cutoff Λ in momentum space. Then the symbol $\int \mathcal{D}^\Lambda \phi$ means integrating from the cutoff Λ to high-momentum. We could rewrite the system as

$$Z = \int \mathcal{D}_\Lambda \phi \int \mathcal{D}^\Lambda \phi e^{-S[\phi]} = \int \mathcal{D}_\Lambda \phi e^{-S_\Lambda[\phi]}, \tag{3.91}$$

where we defined an effective action $S_\Lambda[\phi]$,

$$e^{-S_\Lambda[\phi]} \equiv \int \mathcal{D}^\Lambda \phi e^{-S[\phi]}. \tag{3.92}$$

Generally, physical quantities, such as correlation functions, depend on the cutoff Λ in the path integral form. RG requires that these consequences do not occur by *locally* transforming the action $S[\phi]$:

$$Z = \int \mathcal{D}_\Lambda \phi e^{-S_\Lambda[\phi]} = \int \mathcal{D}_{\tilde{\Lambda}} \phi e^{-S_{\tilde{\Lambda}}[\phi]}, \tag{3.93}$$

where this transformation $S_\lambda[\phi] \to S_{\tilde{\Lambda}}[\phi]$ is called *Renormalzation group*(RG) transformation. Notably, for any system, it is non-trivial whether a suitable RG transformation could be found. [17]

Let us discuss the relationship between RG and critical phenomenon. First, we would like to introduce the RG equation. This equation describes coupling constants g^i to cancel the contribution from changing the cutoff Λ. Now, we consider the action S

$$S = -\int d^D x g^i O_i(x), \tag{3.94}$$

where $O_i(x)$ means a local operator, g^i is coupling constant. From the requirement of RG, the RG equation cloud be given by

$$\frac{\partial g^i}{\partial \log \Lambda} = \beta^i(g^i), \tag{3.95}$$

where $\beta^i(g^i)$ is called the *RG beta function.* This equation means that the RG beta function $\beta^i(g^i)$ can be derived from the RG transformation. The system at critical points has scale invariance, which implies that the RG transformation does not induce non-trivial results. Thus, at critical points, we can require that the RG beta functions of non-trivial scalar fields, with a non-trivial coupling constant g^j, vanish: $\beta^i(g^j) = 0$. The zeros of the beta function g^j_* are called a *fixed-point* of the RG.

Next, we focus on RG transformation in the vicinity of this fixed point and then linearize the RG beta function as

$$\beta^i(g^j) = -\varepsilon^i{}_j(g^j - g^j_*). \tag{3.96}$$

Using the eigevectors g'^i with the eigenvalues λ_i of $\varepsilon^i{}_j$, we rewrite the action S as $\int d^D x g'^i O'_i(x)$, where the scaling dimension of $O'_i(x)$ is $\Delta_i (= D - \lambda_i)$. Moreover, from the RG equation, we obtain

$$g'^i - g'^i_* \propto \Lambda^{-\Delta_i}. \tag{3.97}$$

The features of the field $O'_i(x)$ with the scaling dimension Δ_i are the following. (1) If $\Delta_i > 0$, as the cutoff Λ decreases, the operator $O'_i(x)$ drives away from critical points. In this case, the filed $O'_i(x)$ is called a *relevant* operator. Thus, to access

[17] Also, we could interpret RG as *coarse graining* with respect to integral out the high-wavelength region in the path integral form.

critical points, we have to control external parameters. [18] (2) If $\Delta_i < 0$, as the cutoff λ decreases, the operator $O'_i(x)$ would become a negligible operator and is called a *irrelevant* operator. Thus, this case does not require controlling external parameters and can then reach fixed points by RG transformation. (3) If $\Delta_i = 0$, as the cutoff Λ decreases, the operator $O'_i(x)$ does note change and is called a *marginal* operator. To estimate these effects, we have to calculate a high-order term. Fig. 3.6 is an example of the RG transformation flow.

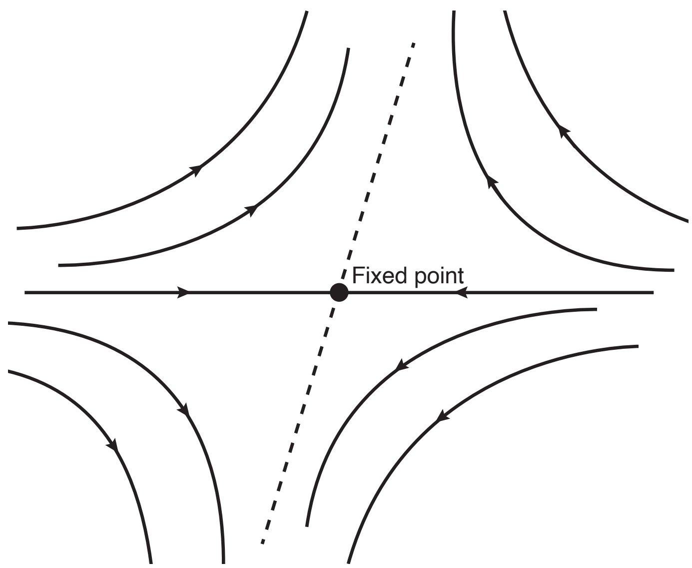

Figure 3.6: Schematic of the RG transformation flow

3.2.2 Zamolodchikov c-theorem

From the RG transformation, we found that the fixed point gives pieces of information on critical phenomena. Now, we would like to discuss how the physics at a fixed point corresponds to CFT in two dimensions. The later discussion proceeds on the method of Zamolodchikov. The current conservation law under the translational transformation is

$$\overline{\partial} T(z,\overline{z}) + \frac{1}{4}\partial\Theta(z,\overline{z}) = 0, \qquad \partial\overline{T}(z,\overline{z}) + \frac{1}{4}\overline{\partial}\Theta(z,\overline{z}) = 0, \tag{3.98}$$

[18]For Cuire transition, these external parameters correspond to temperature and magnetic field.

where Θ can be defined as $\Theta = T^{\mu}{}_{\mu}$ and the conformal weight of Θ is $(h, \overline{h}) = (1, 1)$. [19] Let us consider the two point correlation functions,

$$\langle T(z,\overline{z})T(0,0)\rangle = \frac{F(z\overline{z})}{z^4}, \tag{3.99}$$

$$\langle T(z,\overline{z})\Theta(0,0)\rangle = \langle \Theta(z\overline{z})T(0,0)\rangle = \frac{G(z\overline{z})}{z^3\overline{z}}, \tag{3.100}$$

$$\langle \Theta(z,\overline{z})\Theta(0,0)\rangle = \frac{H(z\overline{z})}{z^2\overline{z}^2}. \tag{3.101}$$

Also, Zamolodchikov proposed the following C-function,

$$C(\tau) = 2F(\tau) + G(\tau) - \frac{3}{8}H(\tau), \tag{3.102}$$

where $\tau = \log(z\overline{z})$. At fixed points, the system possesses the scale invariance, which leads to $\Theta(z, \overline{z}) = 0$ and that this current $T(z, \overline{z})$ become a holomorphic current. Thus, the two point correlation function of the energy-momentum tensor T is

$$\langle T(z)T(0)\rangle = \frac{C/2}{z^4}. \tag{3.103}$$

For two-dimensional CFT, the two point correlation function of the energy-momentum tensor T is

$$\langle T(z)T(0)\rangle = \frac{c/2}{z^4}. \tag{3.104}$$

These results imply that the C-function at fixed points is equal to the central charge c. We found that a system with scale invariance can be described by CFT at fixed points. Generally, systems with scale invariance always possess conformal invariance [121]. However, the generalization of the Zamolodchikov c-theorem turns out to be challenging work and requires concepts from entanglement entropy [122, 123, 124, 125].

3.3 Cardy-Calabrese formula for Entanglement Entropy

Recently, it has been recognized that physics is deeply related to quantum information theory, such as the concept of entanglement entropy [126, 127, 128]. In a

[19] Generally, a field theory can be defined in a manifold. In this case, the traceless condition is not valid. Thus, Θ is a finite value.

quantum system in the state $|\psi_n\rangle$ with probability $p_n(\geq 0)$, the density matrix ρ of this system can be defined as,

$$\rho \equiv \sum_n p_n |\psi_n\rangle \langle\psi_n| , \tag{3.105}$$

where $\sum_n p_n = 1$. Generally, quantum states are classified into two species: pure state and mixed state. For the pure state $|\psi_i\rangle$,

$$p_n = \begin{cases} 1 & n = i \\ 0 & \text{otherwise} \end{cases} , \tag{3.106}$$

and then the density matrix ρ_n is given by $\rho_n = |\psi_n\rangle \langle\psi_n|$. On the other hand, when a density matrix cannot be described as the above form, quantum states correspond to mixed states. In quantum systems, the von Neumann entropy $S(\rho)$ is defined as

$$S(\rho) \equiv - \mathrm{Tr}\left[\rho \ln(\rho)\right] , \tag{3.107}$$

where ρ is a density matrix of quantum systems. This entropy measures the amount of randomness or uncertainty in quantum systems. Obviously, for the pure state $|\psi_n\rangle$, the von Neumann entropy $S(\rho_n)$ is equal to zero. For the later discussion, we assume that the quantum state $|\psi\rangle$ is the pure state.

Next, we would like to discuss quantum entanglement. For a quantum mixed bipartite state $|\psi_{A,B}\rangle$ in Fig. 3.7, the quantum state is separate only if it can be described as the following form,

$$|\psi_{A,B}\rangle = \sum_n \sqrt{p_n} \left|\varphi_n^A\right\rangle \otimes \left|\phi_n^B\right\rangle . \tag{3.108}$$

On the other hand, when the quantum state cannot be described as the above form, it is entangled. The entanglement entropy E_A of a subsystem A is the amount measuring the entanglement between a subsystem A and B, and then is defined as,

$$E_A \equiv S(\mathrm{Tr}_B\left[\rho_{A,B}\right]), \tag{3.109}$$

where $\rho_{A,B} = |\psi_{A,B}\rangle \langle\psi_{A,B}|$ and the symbol of $\mathrm{Tr}_B\left[\cdot\right]$ menas the partial trace of subsystem B. Obviously, an entanglement entropy satisfies $E_A = E_B$.

In general, the entanglement entropy E is the incremental function of a subsystem size L and spatial dimensions d:

$$E(L) \sim L^{d-1}. \tag{3.110}$$

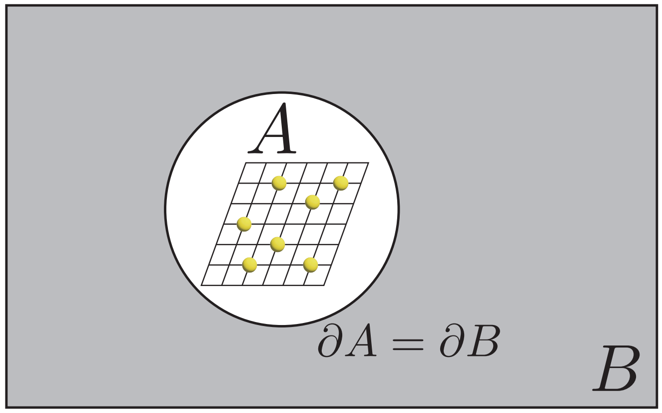

Figure 3.7: Schematic of the subsystem A and B. ∂A means the boundary of the subsystem A.

This consequence is called *Area Law* and is valid under the condition where the correlation length ξ of systems is smaller than the system size L [129]. However, this law is violated in one-dimensional critical systems and systems with Fermi surface [130, 131], and then the entanglement entropy is given by

$$E(L) \sim L^{d-1} \ln L. \tag{3.111}$$

In particular, for one-dimensional critical systems, the entanglement entropy is given by the following formula,

$$E(L) = \begin{cases} \frac{c}{3} \ln \left[\frac{N}{\pi a} \sin \left(\frac{\pi L}{N} \right) \right] + c' & \text{Periodic Boundary,} \\ \frac{c}{6} \ln \left[\frac{2N}{\pi a} \sin \left(\frac{\pi L}{N} \right) \right] + g + c' & \text{Open Boundary,} \end{cases} \tag{3.112}$$

where c' is constant, but non-universal and g is the boundary entropy [126, 127, 132, 133]. Also, this formula is called a *Cardy-Calabrese* formula. We can determine the universality class of systems from the coefficient of entanglement entropy. Thus, the standard method for investigating the universality class is to extract the central charge from the entanglement entropy(Fig. 3.8). In non-Hermitian systems, we only replace the centarl charge c with the effective centarl charge c_{eff}: $c_{\text{eff}} \equiv c - 12(h + \overline{h})$ [135]. However, a naive application of this approach to non-Hermitian systems occasionally leads to some difficulty in numerics [136, 137, 138] as will be discussed in Sec. 4.1.

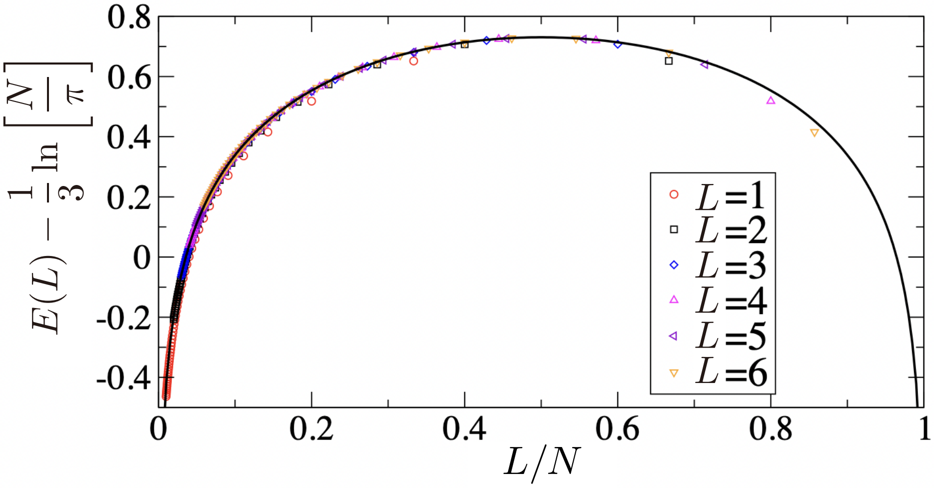

Figure 3.8: Finite size scaling of the entanglement entropy obeying the Cardy-Calabrese formula in antiferromagnetic XXZ chain model [134]. The CFT prediction is that the central charge of this system is equal to $c = 1$, and then the entanglement entropy is $E(L) = \frac{1}{3}\log\left[\sin\frac{\pi L}{N}\right] + \alpha$ under the periodic boundary condition(black line). From the DMRG, $\alpha = 0.7305$.

Chapter 4

non-Hermitian Majorana Systems

In this chapter, we propose a scheme based on a 1D superconductor junction system that realizes the Yang-Lee edge criticality. Our system consists of topological superconducting nanowires coupled with a semiconductor that plays the role of dissipative electron bath. There are Majorana bound states at open ends of 1D topological superconductors. The coupling with electron baths gives rise to the damping of fermion parity for two Majorana bound states, resulting in a non-Hermitian term of the effective Hamiltonian. By using the correspondence between Majorana operators and spin operators, we can map this non-Hermitian Majorana system to the 1D Ising model with an imaginary magnetic field for the Yang-Lee edge singularity.

As mentioned above, this critical state is not topologically protected and not suitable for application to topological quantum computation. However, our proposal has some advantages. In the case of the Read-Rezayi FQH state [42, 43] and superconductor-FQH junction systems [44], in addition to Fibonacci anyons, there are several different types of quasiparticles which are described by the Z_3 parafermion CFT, and it is quite nontrivial how to detect experimentally the topological charge of Fibonacci anyons, discriminating the Fibonacci anyons from other particles. In contrast, in the Yang-Lee edge criticality, there is only one type of a nontrivial particle corresponding to a Yang-Lee anyon, and the field operator for a Yang-Lee anyon is nothing but the scaling limit of the spin magnetization of the non-Hermitian Ising model, which is given by the fermion parity of Majorana bound states in the topological superconductor nanowire system. Thus, the detection and manipulation of Yang-Lee anyons in the nanowire system are more feasible than Fibonacci anyons in the Z_3 parafermion system.

4.1 Yang-Lee model

4.1.1 $\mathcal{PT}$ symmetry

We briefly discuss the features of the Yang-Lee model

$$\mathcal{H}_{\mathrm{YL}} = -\sum_{j=1}^{L} \left[J S_j^z S_{j+1}^z + \Gamma S_j^x + ih S_j^z \right]. \tag{4.1}$$

This model possesses the remarkable symmetry, PT-symmetry, which imposes a typical constraint on the spectrum. To understand this feature, we would like to introduce the parity operator $P = -ie^{i\pi S^x}$ and the time reversal operator $T = \mathcal{K}\Theta$, where $S^x \equiv \sum_{j=1}^{L} S_j^x$, $\mathcal{K}$ is the complex conjugation operator, and Θ, is a unitary operator. Usually, we select the unitary operator Θ as the identity operator $\mathbb{I}$. Let us see the role of these operators. The parity operator P would flip all spins on the yz-plane as

$$\mathcal{P} : (S_j^x, S_j^y, S_j^z) \to (S_j^x, -S_j^y, -S_j^z), \tag{4.2}$$

and the time reversal operator T would only change the y-direction of them as

$$\mathcal{T} : (S_j^x, S_j^y, S_j^z) \to (S_j^x, -S_j^y, S_j^z). \tag{4.3}$$

Thus, the Yang-Lee model $\mathcal{H}_{\mathrm{YL}}$ is $\mathcal{PT}$ invariant, $[PT, \mathcal{H}_{\mathrm{YL}}] = 0$, and is pseudo-hermitian for the parity operator P

$$\mathcal{H}_{\mathrm{YL}}^{\dagger} = P^{-1} \mathcal{H}_{\mathrm{YL}} P. \tag{4.4}$$

From the eigenvalue spectrum theory [46, 139], for systems with pseudo-hermitian, all eigenvalues are real or complex conjugate pairs. Now, let us consider the right eigenstates $|\psi_n\rangle$ with the eigenvalue ϵ_n: $\mathcal{H}_{\mathrm{YL}} |\phi_n\rangle = \epsilon_n |\phi_n\rangle$. [1] Acting on the $\mathcal{PT}$ operator, we obtain $\mathcal{H}_{\mathrm{YL}}(PT|\phi_n\rangle) = \epsilon_n^*(PT|\phi_n\rangle)$. When the eigenstate $|\phi_n\rangle$ is $\mathcal{PT}$ invariant, $(PT|\phi_n\rangle) \propto |\phi_n\rangle$, ϵ_n should be real value. On the other hand, breaking the $\mathcal{PT}$ invariant requires that eigenvalues are complex conjugate pairs. Thus, breaking this symmetry corresponds to the phase transition from real to complex.

[1] In non-Hermitian systems, a biorthogonal basis is much more consistent in calculating expectation values of physical quantities [140, 141].

To see this drastic change in the spectra, we would like to numerically diagonalize the Yang-Lee model by the exact diagonalization method. For $L = 2$, the explicit form of $\mathcal{H}_{\mathrm{YL}}$ is written as

$$\mathcal{H}_{\mathrm{YL}} = -\frac{1}{2}\begin{pmatrix} \frac{J}{2} + 2ih & \Gamma & \Gamma & 0 \\ \Gamma & -\frac{J}{2} & 0 & \Gamma \\ \Gamma & 0 & -\frac{J}{2} & \Gamma \\ 0 & \Gamma & \Gamma & \frac{J}{2} - 2ih \end{pmatrix}. \tag{4.5}$$

The previous study gave the rigorous form of eigenvalues in $\mathcal{PT}$ symmetric phase [142]. As seen Fig. 4.1, the drastic change of spectra occurs by breaking the $\mathcal{PT}$ symmetry

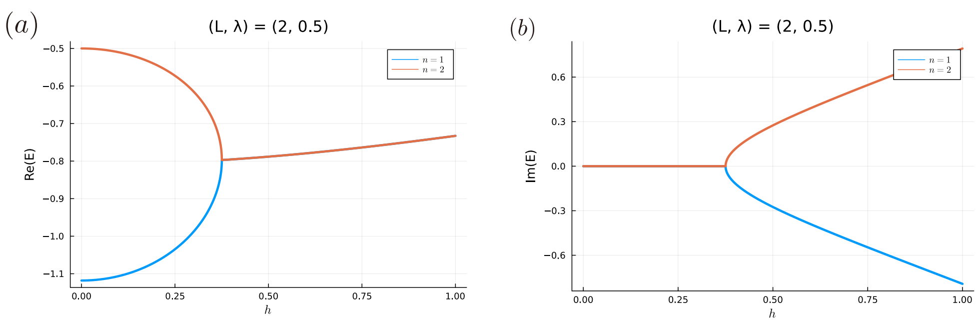

Figure 4.1: The ground state energy ($n = 1$) and the first excited energy ($n = 2$) as a function of magnetic field h.

at the critical magnetic field $h = h_c$, where we define the parameter λ as $\lambda \equiv J/2\Gamma$. Fig. 4.2 shows the phase diagram of the Yang-Lee model $\mathcal{H}_{\mathrm{YL}}$ [113]. The blue area corresponds to the $\mathcal{PT}$-symmetric phase with the real spectra, and the orange area does the $\mathcal{PT}$-broken phase with the complex conjugate pairs spectra. The black line is the critical magnetic field h_c as a function of the parameter λ, and the system shows the Yang-Lee criticality with the central charge $c = -22/5$ on this line.

4.1.2 Non-unitary Behabvior

From the RG method, the magnetization of the Yang-Lee model exhibits a singular behavior with a negative exponent in the vicinity of the critical magnetic field h_c. We can easily check results to imply this consequence. Notably, we found that the magnetization of the first excited state is the opposite value of the magnetization of the ground state. From the CFT, the ground state could host the non-Abelian

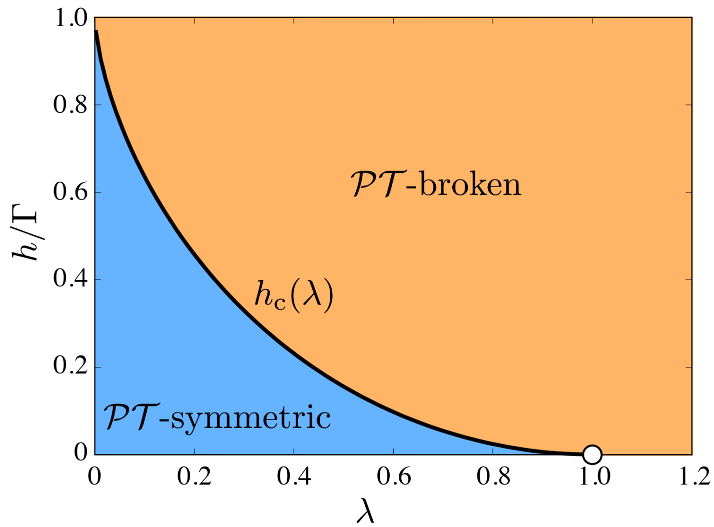

Figure 4.2: The phase diagram of the Yang-Lee model $\mathcal{H}_{\rm YL}$.

anyon τ, and the first excited state could host the trivial vacuum state. Thus, the observation of the magnetization is a strong signature of the non-Abelian anyon τ.

A biorthogonal basis is given by

$$\hat{\mathcal{H}} \left|\phi_n\right\rangle = E_n \left|\phi_n\right\rangle, \left\langle\varphi_n\right| \hat{\mathcal{H}} = E_n \left\langle\varphi_n\right|, \tag{4.6}$$

where $|\phi_n\rangle$ ($\langle\varphi_n|$) is a right (left) eigenstate satisfying $\langle\varphi_n|\phi_m\rangle = \delta_{n,m}$. Also, the observation value of an arbitrary operator $\hat{O}$ could be defined as

$$\langle\hat{O}\rangle_n \equiv \langle\varphi_n|\hat{O}|\phi_n\rangle. \tag{4.7}$$

Fig. 4.3 shows the magnetization $\langle S^z\rangle_n \equiv \langle\varphi_n|S^z|\phi_n\rangle$ as a funciton of the magnetic field h, where $S^z \equiv \sum_{j=1}^{L} S_j^z$. The point where the energy gap is closed corresponds to the singularity of the magnetization $\langle S^z\rangle_n$. This divergent behavior of the magnetization implies the signal of the Yang-Lee edge singularity with a negative exponent. This singularity is an example of non-unitary critical phenomena.

To justify the negative exponent of the magnetization, we numerically calculate the dependence of the system size L. From the phase diagram of the Yang-Lee model $\mathcal{H}_{\rm YL}$, we found that the critical magnetic field $h_c(\lambda)$ strongly depends on the system size L for $\lambda \sim 1.0$. On the other hand, for $\lambda \sim 0.01$, the critical magnetic field $h_c(\lambda)$ is insensitive to change in the system size L. Fig. 4.4(a)-(d) shows the energy gap

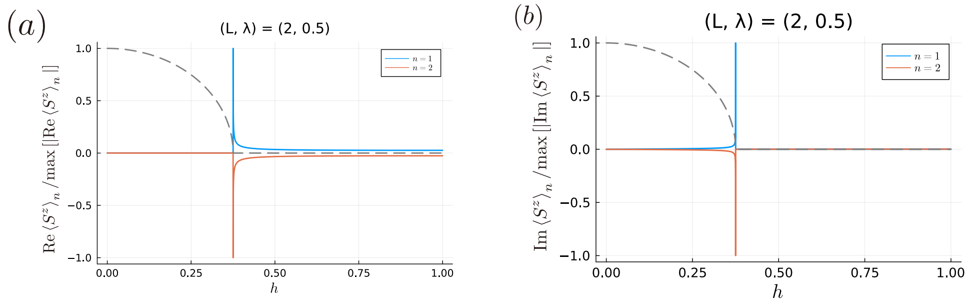

Figure 4.3: The magnetization of the ground state ($n = 1$) and the first excited state ($n = 2$). The dashed line is the real part of the energy gap between the ground state and the first excited state.

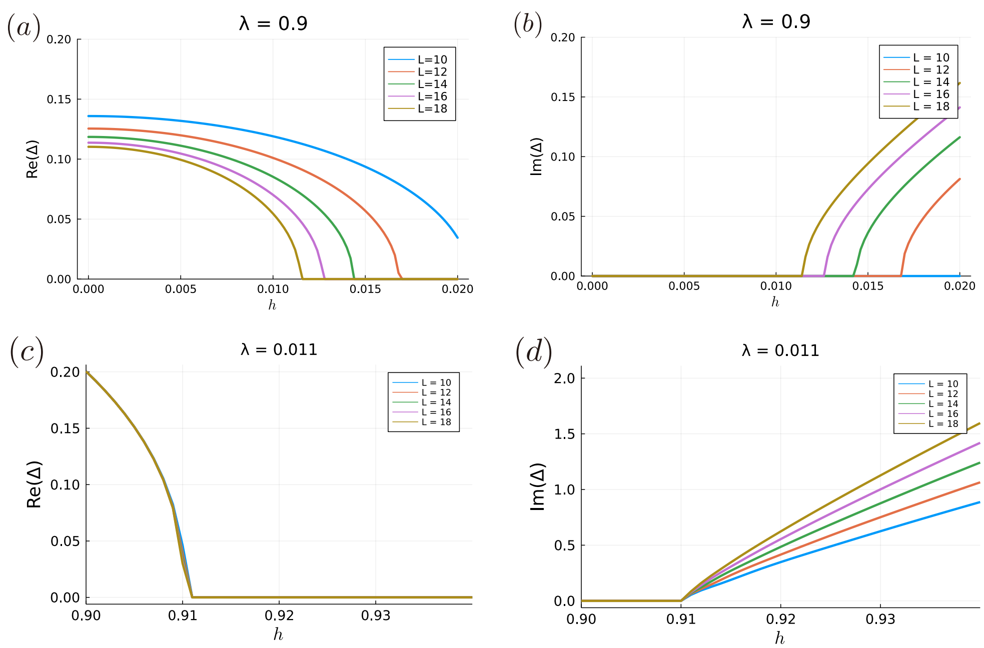

Figure 4.4: The real part and imaginary part of the energy gap between the ground state and the first excited state for $\lambda = 0.9, 0.011$ under the periodic boundary condition.

between the ground state and the first excited state for $\lambda = 0.9, 0.011$ under the periodic boundary condition as the change of the system size L. For $\lambda = 0.9$, the points where the real part of the gap is closed, strongly depend on the system size L. For $\lambda = 0.011$, however, these points are insensitive to change in the system size L. In a finite system, $\lambda \sim 0.01$ is a reasonable scope to numerically calculate the critical behavior.

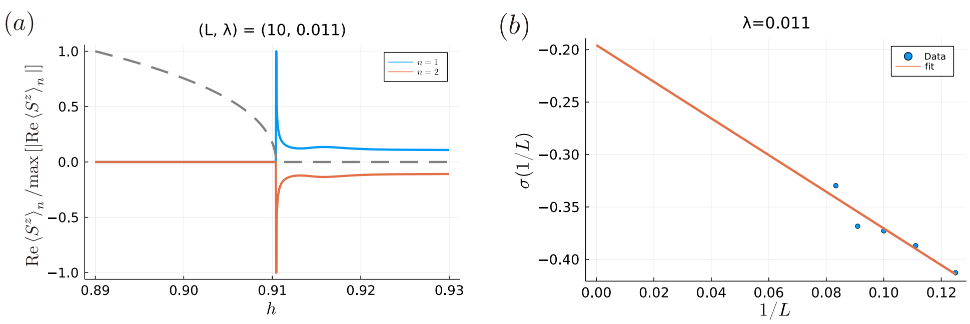

Figure 4.5: (a) The magnetization $\langle S^z \rangle_n$ plotted as a function of h. The blue line $n = 1$ (orange line $n = 2$) corresponds to the ground state (first excited state) in $\mathcal{PT}$-symmetric phase. In the $\mathcal{PT}$-broken phase, the ground state has a negative imaginary part of the spectrum, while the first excited state has a positive imaginary part of that. In these numerical calculations, the maximum value of $|\langle S^z \rangle_n|$ is 13.49 for $n = 1, 2$ at $h = 0.9105$, which implies the divergent behavior of $\langle S^z \rangle_n$ at $h = h_c$. The dashed line is the real part of the energy gap Δ (b) The exponent $\sigma(1/L)$ versus $1/L$. The fitting function is the liner function $\alpha + \beta/L$ with $\alpha = -0.196$ and $\beta = -1.748$.

Fig. 4.5(a) shows the magnetization $\langle S^z \rangle_n$ for $\lambda = 0.011$ plotted as a funciton of h. From the RG method, the negative exponent is theoretically given by $\sigma = -1/6$. Let us check the negative exponet of the magnetization $\langle S^z \rangle_n$ by fitting the field-dependence $\langle S^z \rangle_1 \sim (h - h_c)^\sigma$. Fig. 4.5(b) shows the exponet of $\langle S^z \rangle_1$ as a function of $1/L$. From the intercept of Fig. 4.5(b), we found that $\sigma \approx -0.196$. A finite-size effect often induces this mismatch between numerical and theoretical results. [2] The ground state on the critical line would host the Yang-Lee anyon, and the first excited state is a trivial vacuum state. It is noted that the magnetization for the ground state and for the first excited state show opposite signs. This feature is a complete advantage to detecting the ground state with the Yang-Lee anyons.

[2] For the exact diagonalization method, a finite-size effect is an unavoidable problem.

4.2 non-Hermitian Majorana Systems

In the last section(Sec. 4.1), we have briefly discussed the features of the Yang-Lee model $\mathcal{H}_{\mathrm{YL}}$. The Yang-Lee model $\mathcal{H}_{\mathrm{YL}}$ possesses the $\mathcal{PT}$ symmetry, which imposes that the spectra of this model are real or complex conjugate pairs. It also is noted that the magnetization for the ground state and for the first excited state show opposite signs.

First of all, we would like to transform the Yang-Lee model $\mathcal{M}_{\mathrm{YL}}$ to the Majorana interacting model. We denote the Majorana fields for the remaining three Majorana bound states as γ_j^a, γ_j^b, and γ_j^c. These three Majorana fields constitute an $s = 1/2$ spin operator [143],

$$S_j^x = -\frac{i}{2}\gamma_j^b\gamma_j^c,\ S_j^y = -\frac{i}{2}\gamma_j^c\gamma_j^a,\ S_j^z = -\frac{i}{2}\gamma_j^a\gamma_j^b, \tag{4.8}$$

where these Majorana fields satisfy the anti-commutation relation and $(\gamma_j^\alpha)^\dagger = \gamma_j^\alpha$. The Yang-Lee model $\mathcal{H}_{\mathrm{YL}}$ in the Majorana reperesentation could be written as

$$\mathcal{H}_{\mathrm{YL}}^{\mathrm{MF}} = \sum_j \frac{J}{4}\gamma_j^a\gamma_j^b\gamma_{j+1}^a\gamma_{j+1}^b + \frac{h}{2}\sum_j \gamma_j^a\gamma_j^b + \frac{\Gamma}{2}\sum_j i\gamma_j^b\gamma_j^c. \tag{4.9}$$

The first term is the four-Majorana interaction term, the second term is the damping term of fermion-parity $i\gamma_j^a\gamma_j^b$, and the final term is the hybridization term between γ_j^b and γ_j^c.

Next, We would like to present a scheme for realizing the Yang-Lee model in heterostructure electron systems. Our designed system is constructed from TSC nanowires coupled with metallic substrates, which play the role of electron baths, as shown in Fig. 4.6. The key idea here is that the coupling with electron baths gives rise to a non-Hermitian term associated with dissipations.

Our designed system consists of coupled units, each of which is composed of two TSC nanowires and a nanoscale metallic substrate. In each unit, there are four Majorana bound states at the open edges of the two TSC nanowires. We assume that one of them is sufficiently away from the other three, and its effect is negligible. [3] The Majorana bound states γ_j^b and γ_j^c are coupled via the tunneling term,

$$\mathcal{H}_{\Gamma,j} \equiv \frac{1}{2}\Gamma i\gamma_j^b\gamma_j^c = -\Gamma S_j^x, \tag{4.10}$$

[3] Majorana bound state hybridization between neighboring Majorana bound states lifts the degeneracy from zero energy to finite value[144, 145].

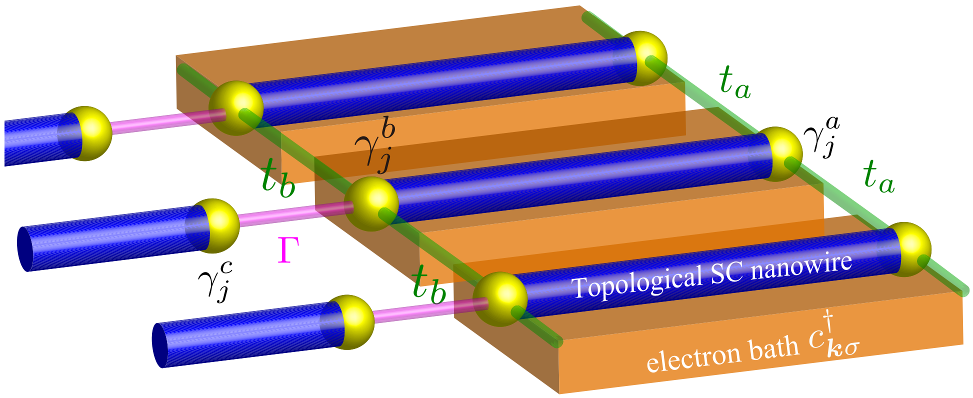

Figure 4.6: Yang-Lee anyon system constructed from Majorana bound states.

which simulates the Zeeman interaction due to a transverse magnetic field.

Furthermore, the Majorana bound states γ_j^a and γ_j^b are coupled to electrons in a nanoscale metallic substrate which plays the role of a dissipative electron bath. The coupling Hamiltonian is given by,

$$\mathcal{H}'_j = \sum_{k,\sigma} iV^a_{k\sigma j}\left(c^\dagger_{k\sigma} + c_{k\sigma}\right)\gamma_j^a + \sum_{k,\sigma} V^b_{k\sigma j}\left(c^\dagger_{k\sigma} - c_{k\sigma}\right)\gamma_j^b \\ + \sum_{k,\sigma} \epsilon_{k\sigma} c^\dagger_{k\sigma} c_{k\sigma}, \tag{4.11}$$

where $c^\dagger_{k\sigma}(c_{k\sigma})$ is a creation (an annihilation) operator of electrons with momentum k, spin σ in the metallic substrate, $\varepsilon_{k\sigma}$ is its energy band, and $V^{a,b}_{k\sigma j}$ are the tunneling amplitudes between Majorana bound states γ_j^a, γ_j^b and the electron bath. To obtain an effective non-Hermitian term corresponding to the imaginary magnetic field of the Yang-Lee model, we switch to the imaginary-time path integral formulation. Since Eq.(4.11) is quadratic in electron fields $c^\dagger_{k\sigma}(c_{k\sigma})$, we can integrate out these fields exactly. Then, we arrive at

$$2\sum_{k,\sigma} V^b_{k\sigma j}\gamma_j^b G_0(\varepsilon_n, k) iV^a_{k\sigma j}\gamma_j^a, \tag{4.12}$$

where $G_0(\varepsilon_n, k) \equiv \frac{1}{i\varepsilon_n - \varepsilon_{k\sigma}}$ is the unperturbed Green function of electrons in the metallic substrate with ε_n the fermionic Matsubara frequency. We apply the analytic continuation of the Matsubara frequency $i\varepsilon_n \to \varepsilon + i\delta$ with δ an infinitesimal quantity, and note $G_0(\varepsilon_n, k) \to \mathrm{P}\left[\frac{1}{\varepsilon - \varepsilon_{k\sigma}}\right] - i\pi\delta(\varepsilon - \varepsilon_{k\sigma})$, where the symbol P [#] means the principal value.

Assuming that k-dependence of $V^{a,b}_{k\sigma j}$ is weak and that the Fermi energy of the substrate is sufficiently large, and the density of states of electrons in the substrate is constant, which justifies the approximation, $\sum_{k,\sigma} \to \int_{-\infty}^{\infty} d\varepsilon_{k\sigma}$, we have $\sum_{k,\sigma} V^b_{k\sigma j} V^a_{k\sigma j} \mathrm{P}\frac{1}{\varepsilon - \varepsilon_{k\sigma}} \approx 0$. Then, we end up with the effective Hamiltonian $\mathcal{H}_{\mathrm{eff}}$ with the damping of fermion parity eigenstate:

$$\begin{aligned} \mathcal{H}_{\mathrm{eff},j} &\sim 2\pi\gamma^a_j\gamma^b_j \sum_{k,\sigma} V^a_{k\sigma j} V^b_{k\sigma j} \delta(\mu - \epsilon_{k\sigma}) \\ &= -ihS^z_j, \end{aligned} \tag{4.13}$$

where $h = 4\pi \sum_{k,\sigma} V^a_{k\sigma j} V^b_{k\sigma j} \delta(\mu - \epsilon_{k\sigma})$, and μ is the Fermi level of the metallic substrate. [4] Eq. (4.13) is indeed non-Hermitian and simulates the Zeeman interaction between an imaginary magnetic field and the z-component of the spin.

We, furthermore, introduce the tunneling term between Majorana bound states in neighboring units,$\gamma^{a(b)}_j$ and $\gamma^{a(b)}_{j\pm1}$:

$$\mathcal{H}_{\mathrm{tun}} = \sum_j \left[it_a\gamma^a_j\gamma^a_{j+1} + it_b\gamma^b_j\gamma^b_{j+1} \right]. \tag{4.14}$$

As shown below, this term generates the Ising interaction between neighboring spins expressed by Majorana fields. We deal with $\mathcal{H}_{\mathrm{tun}}$ as a perturbation to the eigenstates of the Hamiltonian of the decoupled Majorana units $\mathcal{H}_0 = \sum_j [\mathcal{H}_{\mathrm{eff},j} + \mathcal{H}_{\Gamma,j}]$. The eigen energies of each Majorana unit are given by $E_\pm = \pm\frac{1}{2}\sqrt{\Gamma^2 - h^2}$. A key assumption in the following analysis is that the hopping amplitudes of $\mathcal{H}_{\mathrm{tun}}$ are much smaller than $|E_\pm|$, which justifies the perturbative treatment. We consider the correction to the Hamiltonian due to the second order perturbation, $P\mathcal{H}_{\mathrm{tun}}\frac{1}{E_0 - \mathcal{H}_0}\mathcal{H}_{\mathrm{tun}}P$ where E_0 is the eigenenergy of $\mathcal{H}_0$ in the ground state, P is the projection to the ground state. The intermediate state is the excited state of $\mathcal{H}_0$. The single-Majorana tunneling process induced by $\mathcal{H}_{\mathrm{tun}}$ results in the change of the energy $2E_+$. The first order correction due to $\mathcal{H}_{\mathrm{tun}}$ is suppressed for $t_{a,b} \ll 2E_+$. As a result, the second order perturbation with respect to $\mathcal{H}_{\mathrm{tun}}$ leads to a four-body interaction among Majorana

[4] This result is not unusual. One of the examples is an f-electron in itinerant electrons. From the hybridization between f-electron and itinerant electrons, the pole of the Green's function of f-electron are complex. The real part means energy, and the imaginary part yields a broadening of the spectrum of f-electron.

bound states, which simulates the Ising interaction,

$$\sum_j \frac{J}{4}\gamma_j^a\gamma_j^b\gamma_{j+1}^a\gamma_{j+1}^b = -J\sum_j S_j^z S_{j+1}^z, \tag{4.15}$$

where $J \sim t_a t_b/E_+$.

We present the details of the derivation of the four-Majorana interaction term Eq.(4.15). The eigen energies of the unperturbed non-hermite Hamiltonian for the j-th Majorana unite, $\mathcal{H}_{\mathrm{eff},j} + \mathcal{H}_{\Gamma,j}$, are $E_\pm$. The corresponding right eigenstates are

$$|\phi_{j,R,\pm}\rangle = u_\pm |0\rangle + v_\pm |1\rangle\,, \tag{4.16}$$

where

$$u_+ = \sqrt{\frac{1}{2}\left(1 - \frac{ih}{2E_+}\right)}, \quad v_+ = -\sqrt{\frac{1}{2}\left(1 + \frac{ih}{2E_+}\right)}, \tag{4.17}$$

for the eigenenergy E_+, and $u_- = -v_+$, $v_- = u_+$ for the eigenenergy E_-, and $|0\rangle$ and $|1\rangle$ are, respectively, the eigenstates of the fermion occupation number $\psi_j^\dagger\psi_j = \frac{1}{2}(1 + i\gamma_j^a\gamma_j^b)$ for $\psi_j^\dagger\psi_j = 0$ and 1. Here, $\psi_j \equiv (\gamma_j^a + i\gamma_j^b)/2$. Similarly, the left eigenstates are,

$$\langle\phi_{j,L,\pm}| = u_\pm \langle 0| + v_\pm \langle 1|\,. \tag{4.18}$$

These states constitute a biorthogonal system, satisfying $\langle\phi_{j,L,s}|\phi_{j,R,s'}\rangle = \delta_{ss'}$ with $s, s' = +, -$, and completeness:$\sum_{s=+,-} |\phi_{j,R,s}\rangle\langle\phi_{j,L,s}| = 1$.

With the use of the biorthogonal basis, we carry out the second-order perturbative expansion in $\mathcal{H}_{\mathrm{tun}}$, Eq.(4.14). For clarity, we, here, would focus on the term $it_a\gamma_j^a\gamma_{j+1}^a + it_b\gamma_j^b\gamma_{j+1}^b$ which acts on the j-th and $j+1$-th sites. We can define the right and left eigenstates of the unperturbed Hamiltonian for these two sites, respectively, as $|\phi_{R,s}\rangle \equiv |\phi_{j,R,s_j}\rangle \otimes |\phi_{j+1,R,s_{j+1}}\rangle$ and $\langle\phi_{L,s}| \equiv \langle\phi_{j,L,s_j}| \otimes \langle\phi_{j+1,L,s_{j+1}}|$. Exploiting the relations, $\gamma^a|0\rangle = |1\rangle$, $\gamma^a|1\rangle = |0\rangle$, $\gamma^b|0\rangle = i|1\rangle$, and $\gamma^b|1\rangle = -i|0\rangle$, we obtain the second-order perturbation correction to the ground state $|\phi_{R,-}\rangle$,

$$-\frac{t_a t_b}{2E_+}\gamma_j^b\gamma_{j+1}^b\gamma_j^a\gamma_{j+1}^a|\phi_{R,-}\rangle = -\frac{2t_a t_b}{E_+}S_j^z S_{j+1}^z|\phi_{R,-}\rangle\,, \tag{4.19}$$

which leads to the four-Majorana interaction term Eq.(4.15), and hence, the Ising interaction of the Yang-Lee model. It is noted that the second-order corrections of the order $\mathcal{O}(t_a^2)$ and $\mathcal{O}(t_b^2)$ give just constant terms.

Collecting all the terms, we obtain the Majorana Hamiltonian equivalent to the Yang-Lee model,

$$\begin{aligned}\mathcal{H}_{\rm MF} &= \sum_j \frac{J}{4}\gamma_j^a\gamma_j^b\gamma_{j+1}^a\gamma_{j+1}^b + \frac{h}{2}\sum_j \gamma_j^a\gamma_j^b + \frac{\Gamma}{2}\sum_j i\gamma_j^b\gamma_j^c \\ &= \mathcal{H}_{\rm YL}. \end{aligned} \tag{4.20}$$

The above argument implies that J is much smaller than the other energy scales, $J \ll \sqrt{\Gamma^2 - h^2} < \Gamma$. According to the phase diagram of the Yang-Lee model shown in Fig. 4.2, in the case of $\lambda \ll 1$, the criticality appears for $h \sim \Gamma$. Thus, the Yang-Lee edge criticality for this parameter region can be realized for the interacting Majorana fermion system (4.20). For the feasibility of this scenario, it is crucial to suppress the single-Majorana hopping processes in Eq. (4.14). In the following chapter, we examine the stability of the Yang-Lee edge criticality with the central charge $c = -22/5$ against this perturbation (4.14).

Before closing this section, we mention whether the tunnel term (4.14) affects the $\mathcal{PT}$ symmetry of the Yang-Lee model or not. We define the $\mathcal{P}$ symmetry and $\mathcal{T}$ symmetry operations of Majorana fields at the j-site, which are consistent with those of spin operators as follows:

$$\begin{aligned}\mathcal{P} \quad &: \quad \gamma_j^a \to (-1)^j\gamma_j^a,\ \gamma_j^b \to (-1)^{j+1}\gamma_j^b,\ \gamma_j^c \to (-1)^{j+1}\gamma_j^c, \\ \mathcal{T} \quad &: \quad \gamma_j^a \to (-1)^{j+1}\gamma_j^a,\ \gamma_j^b \to (-1)^{j}\gamma_j^b,\ \gamma_j^c \to (-1)^{j+1}\gamma_j^c, \\ &\quad\ \ i \to -i. \end{aligned} \tag{4.21}$$

Actually, according to these transformation rules, the Majorana Hamiltonian $\mathcal{H}_{\rm MF}$ preserves the $\mathcal{PT}$ symmetry. Also, the tunnel term (4.14) is indeed invariant under the $\mathcal{PT}$ symmetry operation obtained from Eq. (4.21). Thus, the perturbations arising from the tunnel term (4.14) do not break the $\mathcal{PT}$ symmetry of the Yang-Lee model.

4.3 Non-unitary non-Abelian statistics

The non-Abelian anyon statistics are detected by the braiding, fusion, and measurement of anyons. We, here, discuss how to implement these operations of Yang-Lee anyons in our Majorana-based system. Generally, braidings of anyons are achieved for chiral fields of CFTs. However, our system is not chiral, but a purely 1D system, which consists of both holomorphic and anti-holomorphic parts of non-trivial fields, if the periodic boundary condition is imposed. Then, the phase changes of these two parts arising from a braiding operation cancel with each other resulting in trivial braidings only, unless one can manipulate these two parts independently, which is not the case in the Yang-Lee Ising model. However, on the other hand, in the case of open boundary condition, all the primary fields are expressed only by the holomorphic part, and the finite size energy spectrum is given by $E = E_0 + \frac{\pi v}{L}(h_{1,2} + n)$ where E_0 is the ground state energy. Thus, τ is regarded as a chiral field with a conformal spin equal to $\exp(-i\pi h_{1,2}) = \exp(i\pi/5)$. We conjecture that the non-trivial field $\hat{\tau}$, in this case, obeys the rule described by the F-symbol (2.24) and the R-matrix (2.25) in Sec. 2.2. On the basis of this argument, we consider an array of open chains of the Yang-Lee model, which are constructed by using the scheme presented in Sec. 4.1. In Fig. 4.7, we show the schematic of the fusion process. The chains are connected with each other through trivial chains, which are also constructed in the same scheme, but gate potentials are tuned to make them in a trivial insulating phase. By controlling the gate potentials, one can change the trivial chains into a topological state supporting Majorana bound states. Then, two Yang-Lee chains connected via a trivial chain can be turned into a single Yang-Lee chain, which realizes the fusion of non-trivial Yang-Lee particles.

The detection of the topological charge of a Yang-Lee anyon can be carried out by the measurement of the "magnetization" S^z of the Yang-Lee chain system. As seen in Sec. 4.1, the sign of $\langle S^z \rangle$ is different between the non-trivial ground state with an anyon τ and the trivial vacuum state (the first excited state). This difference can be utilized for the detection of the state with τ. Furthermore, the magnetization exhibits a divergent behavior near the critical point, as shown in Fig. 4.5 because of the non-unitary feature. This unique behavior may also be useful for experimental detection. The magnetization $S_z = \frac{i}{2}\gamma_a \gamma_b$ in our Majorana-based system is nothing but a fermion parity, and thus, can be measured by the two-terminal conductance measurement [24].

We, finally, comment on how to carry out the braiding operations of Yang-Lee anyons. We consider two different approaches. The first one is the physical transfer of the Yang-Lee anyon state with the use of gate potential control, as proposed for the case of Ising anyons in topological superconductor nanowire systems [146]. By changing trivial regions into a topological state, and vice versa, the region of the Yang-Lee edge criticality can be transferred to other regions(Fig. 4.8). Using Y-shape junctions, as considered in Ref. [146], we can achieve the transposition of two separated Yang-Lee regions The second approach is to use measurement-based braiding. The measurement-based braiding was considered before for general anyon systems [147], and also for Majorana systems [148]. The basic idea is to exploit quantum teleportation induced by projective measurements of topological charges.

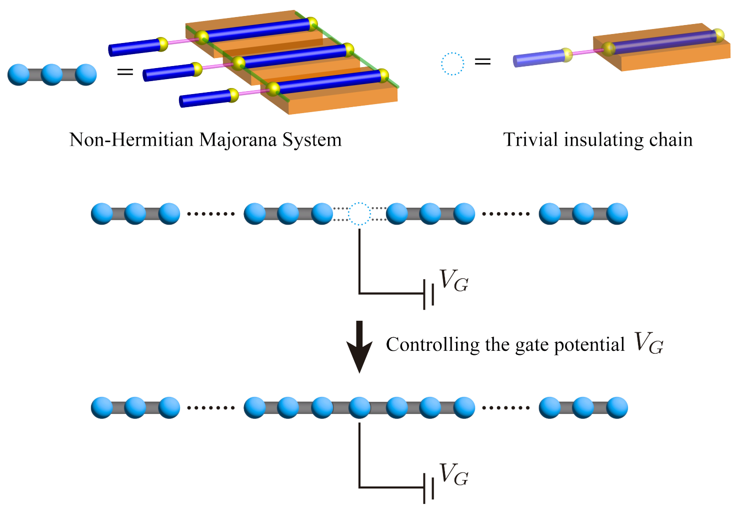

Figure 4.7: Schematics of a fusion process. Two non-Hermitian Majorana systems are connected with each other through a trivial chain. By controlling the gate potential, this trivial chain can host Majorana bound states. Thus, two Yang-Lee chains can be fused into a single Yang-Lee chain.

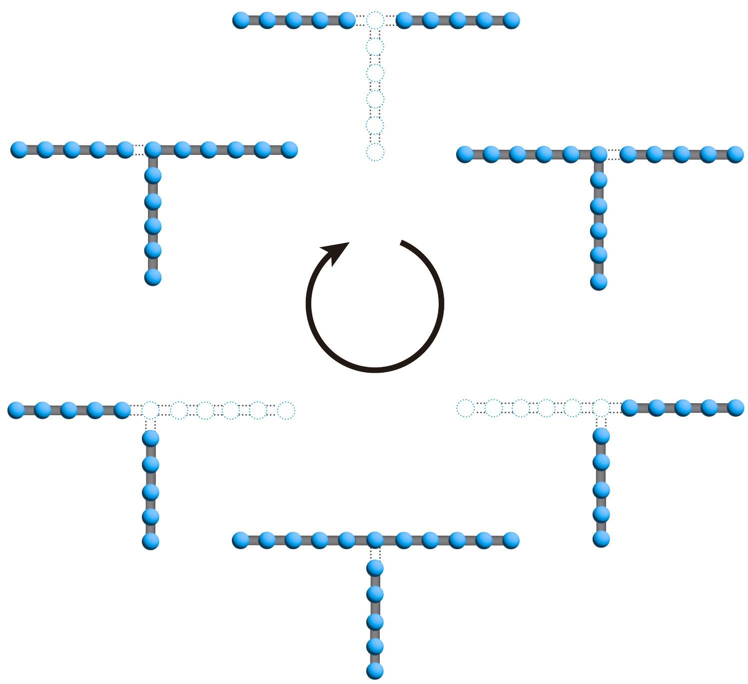

Figure 4.8: Schematics of a braiding process. By controlling the gate potentials, the region of the Yang-Lee edge criticality can be transferred to other regions, as proposed for the case of Majorana qubits.

Following Ref. [147], we apply a sequence of projective measurements of the topological charge, using the above-mentioned procedure, until we obtain desired results, which leads to the transfer of the state with an anyon. Applying this measurement-based transfer to two anyons, one can realize the braiding of them.

4.4 Numerical results

In this section, We would like to discuss the stability of the Yang-Lee edge criticality against the single-Majorana hopping term (4.14) via numerical simulations. The universality class is characterized by the central charge $c = -22/5$ and the scaling dimension $\Delta = -2/5$ of the primary field $\hat{\tau}$. A standard method for the calculation of the central charge is to extract it from the prefactor of the entanglement entropy [126, 127, 135, 136, 137, 138]. However, a naive application of this approach to non-Hermitian systems occasionally leads to some difficulty in numerics. In this thesis, numerical results were obtained by exact diagonalization. We expect it to be accurate enough to evaluate the central charge c and scaling dimensions Δ from the energy spectrums. [5] Thus, we exploit the finite-size scaling method combined with the numerical exact diagonalization.

4.4.1 Yang-Lee edge criticality

We, first, check the Yang-Lee Edge criticality without the Majorana hopping term. There are two methods to estimate the universality class of the system directly. One of them is to extract the central charge c from the coefficient of the entanglement entropy. Recently, this method is well known as a standard method for the estimation of the universality class. We only calculate the ground state of the system, without doing other spectra and excited states.

On the other hand, another method is to extract the central charge from the coefficient of spectra of the system. From the finite-size scaling, we could extract the central charge from the coefficient of the ground state energy per size E_{gs}/L. However, this coefficient includes the velocity of the low-energy excitation. Thus, we have to calculate the energy of some excited states.

[5] There are several numerical methods, such as Time-Evolving Block Decimation, Density Matrix Renormalization Group, and Multi-scale Entanglement Renormalization Ansatz, which need to be adapted to our system when discussing the thermodynamic limit, which is an unavoidable challenge when observing the signal of Yang-Lee anyon. Our recent study can estimate the exponent of the magnetization in thermodynamic limit [149].

Entanglement Entropy

We examine the Cardy-Calabrese formula for entanglement entropy in the case of the Yang-Lee edge criticality. For the unitary case, the Cardy-Calabrese formula is quite successful for obtaining the central charge [126, 127]. In the case of non-unitary CFTs, it was conjectured that the central charge in the prefactor of the entanglement entropy $S(L)$ for the system size L is replaced with an effective central charge,

$$S(L) = \frac{c_{eff}}{3} \log \frac{L}{\epsilon} + \mathcal{O}(1) \tag{4.22}$$

where ϵ is a non-universal ultraviolet cut-off [135, 137, 138]. Here, the periodic boundary condition is imposed.

For the Yang-Lee model, the effective central charge was numerically examined by using Eq. (4.22) [136]. In the previous study [136], the entanglement entropy was calculated for the parameter $\lambda = 0.9$. On the other hand, we used much smaller values of the parameter $\lambda \sim 0.01$ to ensure the stability of numerical calculations against the change of the system size, which is necessary for the numerical calculations in the case of the interacting Majorana model. Also, our construction of the Yang-Lee system with Majorana bound states is applicable for small λ. For this parameter region, the non-Hermitian term, i.e. the imaginary magnetic field, dominates over the Ising interaction term, leading to the situation that the deviation from the Cardy-Calabrese formula for the non-unitary case is serious if the system size is not large enough.

To demonstrate this, we calculate the entanglement entropy for the non-Hermitian system by using the biorthogonal basis. That is, the density matrix ρ is defined as $\rho \equiv |\varphi\rangle \langle\phi|$, where $|\varphi\rangle$ ($\langle\phi|$) is the right (left) eigenvector of the non-Hermitian Hamiltonian. Then, we divide the system into two parts, i.e. system A and system B. The entanglement entropy of subsystem A is $S_A = \mathrm{Tr}\left[\rho_A \log \rho_A\right]$ where ρ_A is the reduced density matrix of system A by tracing out system B: $\rho_A = \mathrm{Tr}_B\left[\rho\right]$. In Fig. 4.9, we show the calculated results of the real part of the entanglement entropy. From Fig. 4.9 (b), we estimate the effective central charge $c_{eff} \sim 0.889$, which is inconsistent with the theoretical prediction $c_{eff} = 0.4$. This slow convergence is due to the logarithmic dependence on the system size (4.22).

To obtain the correct value of the central charge for this non-Hermitian term dominated region, we need to carry out calculations for much larger system sizes, which require high numerical costs. The result indicates that the numerical calculations of the entanglement entropy for non-Hermitian systems require much larger system sizes than hermitian systems, when non-Hermitian terms are predominant.

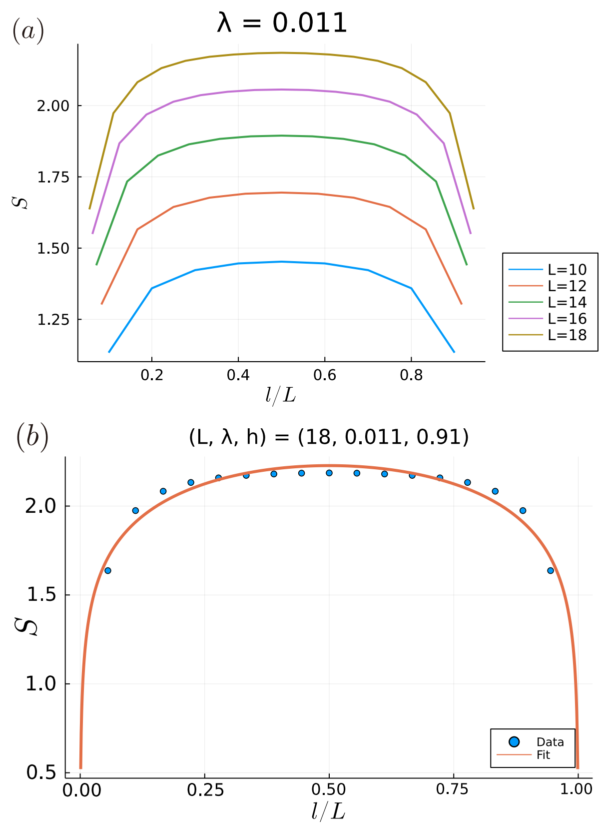

Figure 4.9: (a) Entanglement Entropy in the vicinity of the Yang-Lee critical point. (b) Entanglement Entropy for $L = 18$. The fitting function is $\frac{\alpha}{3}\log\left[\frac{L}{\pi}\sin\left(\frac{\pi l}{L}\right)\right] + \beta$ with $\alpha = 0.889$ and $\beta = 1.711$.

Because of this reason, we exploit the finite size scaling method for the calculation of the central charge in the next section.

Finite Size Scaling

We present the details of the method for numerical calculation. It is noted that the Yang-Lee edge criticality corresponds to an exceptional point of the non-Hermitian Hamiltonian, and thus, we need to handle numerical diagonalization in the vicinity of the critical point with special care. We can easily estimate the critical magnetic field h_c from the drastic change of energy spectra at h_c.

For finite size scaling and Virasoro operator $L_n, \overline{L}_n$, Hamiltonian at criticality is, for the periodic boundary condition (P.B.C.), given by

$$\mathcal{H} = \epsilon_0 L - \frac{\pi v}{6L} c + \frac{2\pi v}{L} \left[L_0 + \overline{L}_0 \right], \tag{4.23}$$

where ϵ_0 is the energy density, L is the system size, c is the central charge of the system, and v is the velocity of the low-energy excitation [88]. The non-unitary CFT for the Yang-Lee edge singularity is the minimal model $\mathcal{M}_{5,2}$ with the central charge $c = -22/5$ and the scaling dimension $\Delta = -2/5$ for the only one non-trivial field, For $p = 5, q = 2$, there are two primary fields:

$$\begin{cases} \text{trivial field } \hat{\mathbb{I}} & h_{1,1} = h_{1,4} = 0, \\ \text{non-trivial field } \hat{\tau} & h_{1,2} = h_{1,3} = -1/5, \end{cases} \tag{4.24}$$

and then anti-holomorphic parts could be defined similarly. Thus, the energy spectra of the Yang-Lee model at criticality are, for P.B.C., given by

$$E^{\hat{\mathbb{I}}}(n, \overline{n}) = \epsilon_0 L - \frac{\pi v}{6L} c + \frac{2\pi v}{L} (n + \overline{n}), \tag{4.25}$$

$$E^{\hat{\tau}}(n, \overline{n}) = \epsilon_0 L - \frac{\pi v}{6L} c_{\text{eff}} + \frac{2\pi v}{L} (n + \overline{n}), \tag{4.26}$$

, where we define the scaling dimension Δ: $\Delta \equiv h_{1,2} + \overline{h}_{1,2}$ and the effective central charge c_{eff}: $c_{\text{eff}} \equiv c - 12\Delta$. Thus, the physical ground state $|\text{gs}\rangle$ is the primary state $|h, \overline{h}\rangle$ with the conformal weights $(h, \overline{h}) = (-1/5, -1/5)$, and the energy level $E^{\hat{\tau}}(0, 0)$. The first excited state $|1\text{st}\rangle$ is the trivial primary state $|0, 0\rangle$ with the conformal weights $(0, 0)$ and the energy level $E^{\hat{\mathbb{I}}}(0, 0)$. Alos, the second excited state $|2\text{nd}\rangle$ is the level 1 descendant state of the ground state $|\text{gs}\rangle$ expressed as,

$$|2\text{nd}\rangle \sim L_{-1} |\text{gs}\rangle \text{ or } \overline{L}_{-1} |\text{gs}\rangle . \tag{4.27}$$

The energy levels of the second excited state are given by $E^{\hat{\tau}}(1,0)$ and $E^{\hat{\tau}}(0,1)$. From the energy spectrum obtained by using exact diagonalization, we obtain the central charge c, the scaling dimension Δ and the velocity v.

We check that the critical behavior predicted from the CFT is actually realized at the numerically determined h_c as shown below. As seen in Fig. 4.2, the numerical values of $h_c(\lambda)$ are not sensitive to the change of the system size L for $\lambda \sim 0.01$. On the other hand, h_c strongly depends on the system size for larger values of λ, e.g., ~ 1.0. For the non-Hermitian interacting Majorana model given in Sec. 4.2, there is redundant degeneracy $2^{L/2}$ because of the Majorana representation [143], and thus, the Hilbert space is much larger than the case of the Yang-Lee spin model, which makes it difficult to carry out numerical calculations for large system sizes. Because of this reason, we select the parameter J corresponding to $\lambda \sim 0.01$ with $\Gamma = 1$, for which the dependence of h_c on L is weak.

We, first, determine h_c numerically from the behavior of the first excited energy gap Δ_1. In Fig. 4.4(c)(d), we show the energy gap Δ_1 for $\lambda = 0.011$. From this figure, we see that the critical magnetic field $h_c(\lambda)$ is around $h = 0.910$ for this parameter. For $8 \leq L \leq 18$, the real and imaginary parts of Δ_1 exhibit drastic changes, which indicates the $\mathcal{PT}$ symmetry breaking around $h = 0.910$.

We, next, check for the criticality of the Yang-Lee model as a function of a magnetic field h. We define the function $F(h)$:

$$F(h) \equiv \frac{E_{\rm 1st}(h) - E_{\rm gs}(h)}{E_{\rm 2nd}(h) - E_{\rm gs}(h)} + \Delta, \tag{4.28}$$

where $E_{\rm gs}$, $E_{\rm 1st}$, and $E_{\rm 2nd}$ are, respectively, the energy levels for the ground state, the first excited state, and the second excited state. The function $F(h)$ must be zero on the Yang-Lee Edge criticality, and is useful for identifying the critical point. In Fig.4.10, we plot the function $F(h)$ for $0.9 \leq h \leq 0.910$. From this figure, we can expect that the region in the vicinity of $h = 0.910$ is on the Yang-Lee Edge criticality.

We, further, examine the universality class of criticality by using the finite size scaling method. The finite size energy spectra of the Yang-Lee CFT are given by Eqs. (4.25)-(4.26). The first step is to fit the spectra with the function form,

$$\frac{E}{L} = a + \frac{b}{L^2}, \tag{4.29}$$

and obtain the velocity v from the relation $2\pi v = b_{\rm 2nd} - b_{\rm GS}$. The second step is to calculate the central charge c by substituting the velocity v into $-6b_{\rm 1st}/\pi v$. The final step is to estimate the scaling dimension Δ by using the above results for $b_{\rm 2nd} = 2\pi v - \pi v c_{\rm eff}/6$. In Fig. 4.11, we show the fitting of numerical data

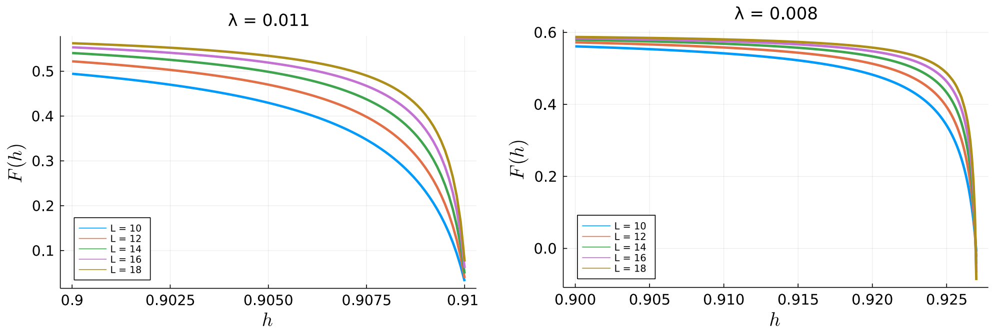

Figure 4.10: The function $F(h)$ versus h

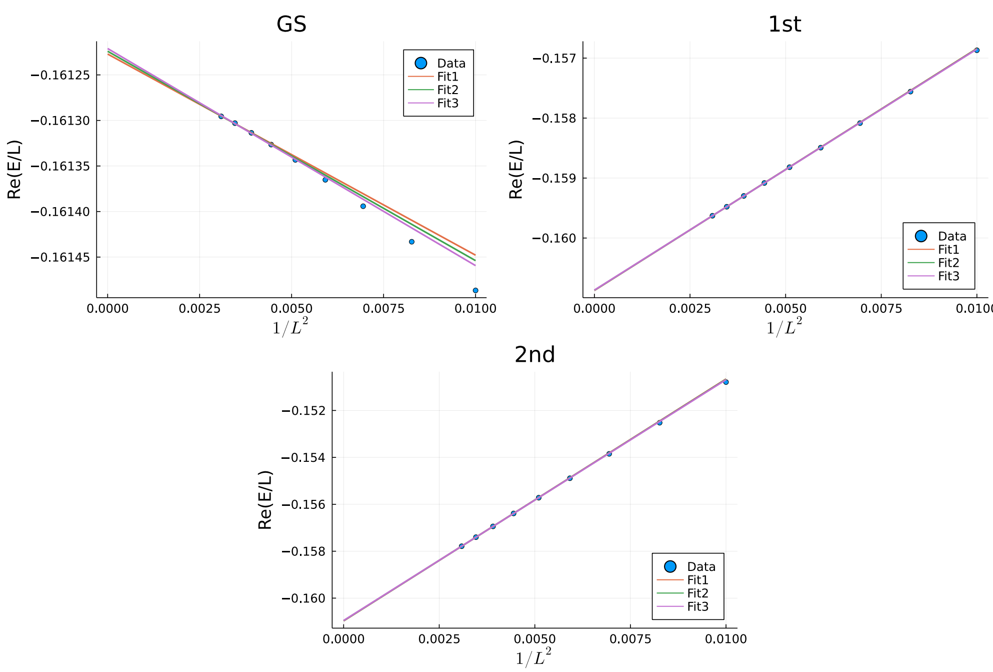

Figure 4.11: The energy levels of the ground state, the first excited state, and the second excited state for $\lambda = 0.011$. Fit.1 is a fitting function obtained from data for $L = 18, 16, 14$. Fit.2 is obtained from data for $12 \leq L \leq 18$, and Fit.3 is obtained by using all of them.

$\lambda = 0.011$	c	Δ	$\lambda = 0.008$	c	Δ
Fit 1	-4.5889	-0.4050	Fit 1	-4.4859	-0.4278
Fit 2	-4.5909	-0.4072	Fit 2	-4.5186	-0.4272
Fit 3	-4.6054	-0.4106	Fit 3	-4.5522	-0.4264

Table 4.1: Central charge c and scaling dimension Δ. Yang-Lee edge criticality has the central charge $c = -4.4$ and the scaling dimension $\Delta = -0.4$. Fit.1 is a fitting function obtained from data for $L = 18, 16, 14$. Fit.2 is that for $12 \leq L \leq 18$, and Fit.3 is obtained by using all of these data.

of the energy spectra to the function (4.29). The numerical data well satisfy the finite size energy spectra in Eqs. (4.25)-(4.26), implying that the criticality is described by the Yang-Lee edge CFT. As a result, we set the parameters as $(\lambda, h) = (0.011, 0.910), (0.008, 0.927)$. From the finite-size scaling and fitting method, we numerically estimate the central charge and the conformal weight (Tab. 4.1). Numerical results imply that the universality class of the criticality for these parameters coincides with the Yang-Lee edge singularity.

4.4.2 Stability of the Yang-Lee edge criticality

In the last section, we numerically estimated the universality class of the Yang-Lee model $\mathcal{H}_{\mathrm{YL}}$ in the spin system. These results show the Yang-Lee edge criticality with the central charge $c = -22/5$ and the scaling dimension $\Delta = -2/5$. Our designed non-Hermitian Majorana systems would be valid in the case where the single-Majorana hopping processes are sufficiently smaller than other parameters.

First of all, we examine the effect of the single-Majorana hopping processes against the Yang-Lee model. Let us consider the following Hamiltonian in Majorana representation,

$$\mathcal{H}_{\mathrm{total}} = \mathcal{H}_{\mathrm{MF}} + \mathcal{H}'_{\mathrm{MF}} \tag{4.30}$$

$$\mathcal{H}_{\mathrm{MF}} = \sum_j \frac{J}{4}\gamma_j^a\gamma_j^b\gamma_{j+1}^a\gamma_{j+1}^b + \frac{h}{2}\sum_j \gamma_j^a\gamma_j^b + \frac{\Gamma}{2}\sum_j i\gamma_j^b\gamma_j^c \tag{4.31}$$

$$\mathcal{H}'_{\mathrm{MF}} = \sum_j \left[it\gamma_j^a\gamma_{j+1}^a + it\gamma_j^b\gamma_{j+1}^b\right]. \tag{4.32}$$

For $t = 0$, each state is redundant degeneracy $2^{L/2}$. In Sec. 4.2, we mentioned that the single-Majorana hopping processes $\mathcal{H}'_{\mathrm{MF}}$ do not break the $\mathcal{PT}$ symmetry of the Yang-Lee model. However, the single-Majorana hopping processes can flip the local fermion parity between j-site and $j+1$-site: $|\cdots,0,1,\cdots\rangle \rightarrow |\cdots,1,0,\cdots\rangle$. Thus, this hopping process could split the degeneracy states. Moreover, Fig. 4.12 shows the

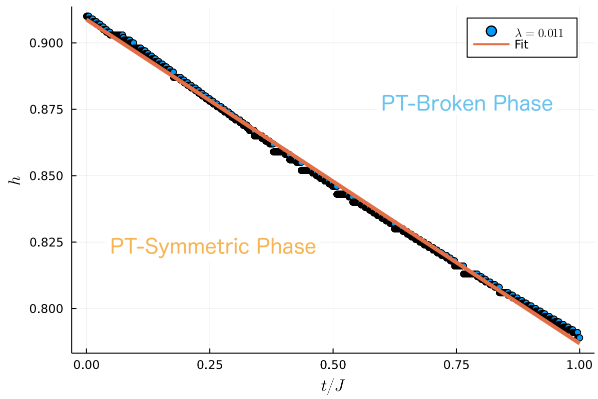

Figure 4.12: Numerical data of critical magnetic field h_c for $\lambda = 0.011$ as a function of t/J. The orange line is the fitting line. Numerical data show that the single-Majorana hopping processes can shift the critical magnetic field h_c.

phase diagram of the Hamiltonian $\mathcal{H}_{\text{total}}$. As seen in Fig. 4.12, the single-Majorana hopping processes $\mathcal{H}'_{\text{MF}}$ can shift the critical magnetic field h_c.

In Fig. 4.13, we show the central charge c and the scaling dimension Δ versus the amplitude of the Majorana hopping term. It is found that the Yang-Lee edge criticality is stable up to $t/J \sim 10^{-4}$. The results indicate that the criticality is stable as long as the Majorana hopping term is sufficiently suppressed.

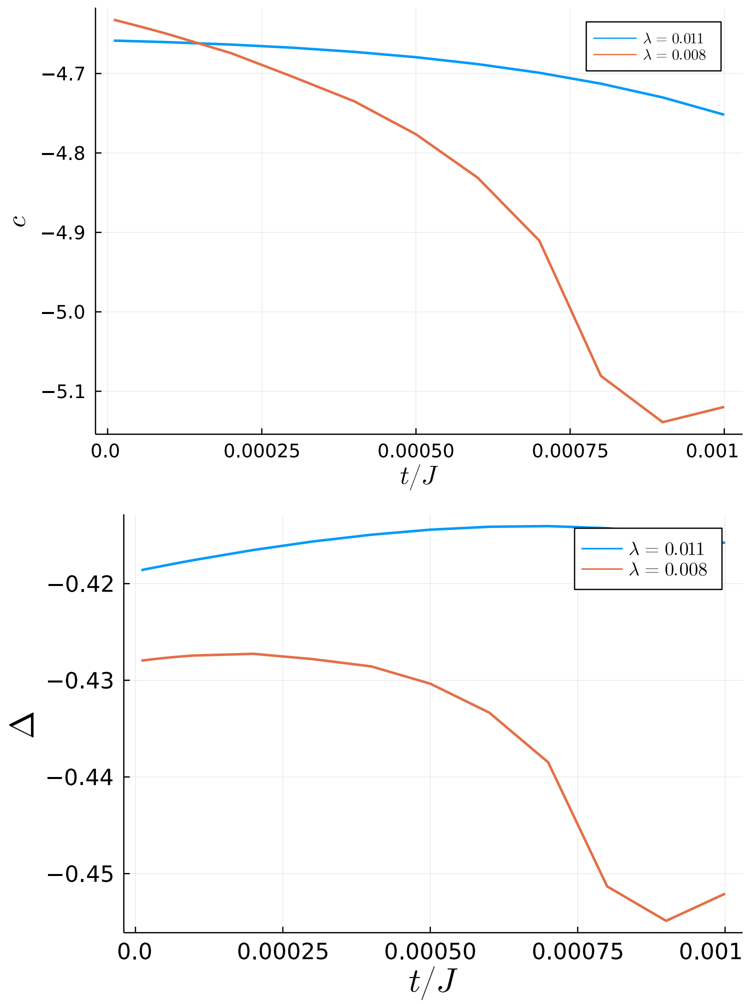

Figure 4.13: Central charge c and scaling dimension Δ of the nontrivial primary field for the non-Hermitian Majorana system with the single Majorana hopping term $\mathcal{H}_{\mathrm{MF}} + \mathcal{H}_{\mathrm{tun}}$ plotted as a function of the hopping amplitude t/J. The blue line is the case of $\lambda = 0.011$, and the red line is that of $\lambda = 0.008$.

Chapter 5

Summary

In this thesis, we design the platform for Yang-Lee anyons which are non-unitary counterparts of Fibonacci anyons, obeying the same fusion rule. Our proposed system is a non-Hermitian interacting Majorana system constructed from the 1D TSC junctions coupled with dissipative electron baths, which can simulate the Yang-Lee edge criticality. The coupling with electron baths gives rise to the damping of fermion parity in a superconducting nanowire, which plays the role of an imaginary magnetic field in terms of spin representation. On the other hand, the setup based on Majorana quasiparticles means that the observation of Yang-Lee anyon is a direct probe of Majorana quasiparticles. To stabilize the Yang-Lee edge criticality, it is important to suppress single-Majorana hopping processes in the junction system, which do not exist in the Yang-Lee spin model. We can decrease these undesirable processes by tuning system parameters. We also present the scheme for the braiding, fusion, and detection of Yang-Lee anyons in our TSC junction system.

In the Yang-Lee edge criticality, which is described by the non-unitary CFT with the central charge $c = -22/5$, the ground state is the non-trivial state corresponding to a Yang-Lee anyon, while the first excited state is a trivial vacuum. Because of the non-unitary character of the CFT, the non-Abelian braiding operator of Yang-Lee anyons is non-unitary, leading to non-unitary non-Abelian statistics. Although it is not suitable for application to unitary quantum computation, it may be utilized for simulating non-unitary quantum dynamics in a controllable way. Our study suggests that non-Hermitian Majorana many-body systems embrace rich physics inherent in open quantum systems and can be realized by exploiting topological superconductor junction systems in a feasible and controllable way. It is an interesting future issue to explore for further exotic phases emerging from non-Hermitian Majorana many-body systems.

List of Publications

Papers

1. Takumi Sanno, Shunsuke Miyazaki, Takeshi Mizushima, and Satoshi Fujimoto, "*Ab initio simulation of non-Abelian braiding statistics in topological superconductors*", Phys. Rev. B **103**, 054504 (2021).

2. Yuki Tanaka, Takumi Sanno, Takeshi Mizushima, and Satoshi Fujimoto, "*Manipulation of Majorana-Kramers qubit and its tolerance in time-reversal invariant topological superconductor*", Phys. Rev. B **106**, 014522 (2022), as the corresponding author.

3. Takumi Sanno, Masahiko G. Yamada, Takeshi Mizushima, and Satoshi Fujimoto, "*Engineering Yang-Lee anyons via Majorana bound states*", Phys. Rev. B **106**, 174517 (2022).

Preprints

1. Masahiko G. Yamada, Takumi Sanno, Masahiro O. Takahashi, Yutaka Akagi, Hidemaro Suwa, Satoshi Fujimoto, and Masafumi Udagawa, "*Matrix Product Renormalization Group: Potential Universal Quantum Many-Body Solver*", arXiv:2212.13267(submitted to Physical Review Letters).

Acknowledgment

I thank Manato Fujimoto, Satoshi Fujimoto, Kenichi Kasamatsu, Hiroaki Kato, Yoshiteru Maeno, Taiki Matsushita, Takeshi Mizushima, Yuki Nagai, Mikio Nakahara, Nobuyoshi Ohta, Masahiro O. Takahashi, Daichi Takikawa, Atsushi Tsuruta, Masahiko G. Yamada, and Tomohiro Yamazaki for the fruitful discussion and comments on my research. I am supported by a JSPS Fellowship for Young Scientists. A part of the computation in this thesis has been done using the facilities of the Supercomputer Center, the Institute for Solid State Physics, and the University of Tokyo.

I am grateful to Satoshi Fujimoto, Takeshi Mizushima, and Atsushi Tsuruta for their education and encouragement during my master's and doctor's course. Thanks to their deep knowledge of condensed matter physics, I have learned and studied topological systems and non-Abelian anyons. I think that I definitely cannot do that without their support. Fujimoto's lab members often entertained and discussed with me. I really hope that they take condensed matter physics by storm.

Also, my friends always encourage and cheer me when I am worried or troubled. I appreciate my friend's support. Sometimes, they had dinner with me, and Sometimes they chatted with me, and many more.

Finally, I express gratitude to my family for their continuous support and encouragement.

Bibliography

[1] F. Wilczek, *Quantum Mechanics of Fractional-Spin Particles,* Phys. Rev. Lett. **49**, 957 (1982).

[2] D. C. Tsui, H. L. Stormer, and A. C. Gossard, *Two-Dimensional Magnetotransport in the Extreme Quantum Limit,* Phys. Rev. Lett. **48**, 1559 (1982).

[3] R. B. Laughlin, *Anomalous Quantum Hall Effect: An Incompressible Quantum Fluid with Fractionally Charged Excitations,* Phys. Rev. Lett. **50**, 1395 (1983).

[4] G. Moore and N. Read, *Nonabelions in the fractional quantum hall effect,* Nucl. Phys. B **360**, 362 (1991).

[5] N. Read and D. Green, *Paired states of fermions in two dimensions with breaking of parity and time-reversal symmetries and the fractional quantum Hall effect,* Phys. Rev. B **61**, 10267 (2000).

[6] D. A. Ivanov, *Non-Abelian Statistics of Half-Quantum Vortices in p-Wave Superconductors,* Phys. Rev. Lett. **86**, 268 (2001).

[7] A. Kitaev, *Anyons in an exactly solved model and beyond,* Ann. Phys. **321**, 2 (2006).

[8] M. H. Freedman, M. Larsen, and Z. Wang, *A Modular Functor Which is Universal for Quantum Computation,* Commun. Math. Phys. **227**, 605 (2002).

[9] M. Freedman, A. Kitaev, M. Larsen, and Z. Wang, *Topological quantum computation,* Bull. Amer. Math. Soc. **40**, 31 (2003).

[10] C. Nayak, S. H. Simon, A. Stern, M. Freedman, and S. Das Sarma, *Non-Abelian anyons and topological quantum computation,* Rev. Mod. Phys. **80**, 1083 (2008).

[11] S. Bravyi and A. Kitaev, *Universal quantum computation with ideal Clifford gates and noisy ancillas,* Phys. Rev. A **71**, 022316 (2005).

[12] S. Bravyi, *Universal quantum computation with the* $\nu = 5/2$ *fractional quantum Hall state,* Phys. Rev. A **73**, 042313 (2006).

[13] L. S. Georgiev, *Topologically protected gates for quantum computation with non-Abelian anyons in the Pfaffian quantum Hall state,* Phys. Rev. B **74**, 235112 (2006).

[14] S. Bravyi, B. M. Terhal, and B. Leemhuis, *Majorana fermion codes,* New J. Phys. **12**, 083039 (2010).

[15] H. Xu and X. Wan, *Constructing functional braids for low-leakage topological quantum computing,* Phys. Rev. A **78**, 042325 (2008).

[16] H. Xu and X. Wan, *Exploiting geometric degrees of freedom in topological quantum computing,* Phys. Rev. A **80**, 012306 (2009).

[17] P. Bonderson, D. J. Clarke, C. Nayak, and K. Shtengel, *Implementing Arbitrary Phase Gates with Ising Anyons,* Phys. Rev. Lett. **104**, 180505 (2010).

[18] F. Hassler, A. R. Akhmerov, and C. W. J. Beenakker, *The top-transmon: a hybrid superconducting qubit for parity-protected quantum computation,* New J. Phys. **13**, 095004 (2011).

[19] B. van Heck, A. R. Akhmerov, F. Hassler, M. Burrello, and C. W. J. Beenakker, *Coulomb-assisted braiding of Majorana fermions in a Josephson junction array,* New J. Phys. **14**, 035019 (2012).

[20] T. Hyart, B. van Heck, I. C. Fulga, M. Burrello, A. R. Akhmerov, and C. W. J. Beenakker, *Flux-controlled quantum computation with Majorana fermions,* Phys. Rev. B **88**, 035121 (2013).

[21] S. Vijay, T. H. Hsieh, and L. Fu, *Majorana Fermion Surface Code for Universal Quantum Computation,* Phys. Rev. X **5**, 041038 (2015).

[22] L. A. Landau, S. Plugge, E. Sela, A. Altland, S. M. Albrecht, and R. Egger, *Towards Realistic Implementations of a Majorana Surface Code,* Phys. Rev. Lett. **116**, 050501 (2016).

[23] D. Aasen, M. Hell, R. V. Mishmash, A. Higginbotham, J. Danon, M. Leijnse, T. S. Jespersen, J. A. Folk, C. M. Marcus, K. Flensberg, and J. Alicea, *Milestones Toward Majorana-Based Quantum Computing,* Phys. Rev. X **6**, 031016 (2016).

[24] S. Plugge, L. A. Landau, E. Sela, A. Altland, K. Flensberg, and R. Egger, *Roadmap to Majorana surface codes,* Phys. Rev. B **94**, 174514 (2016).

[25] C. Knapp, M. Beverland, D. I. Pikulin, and T. Karzig, *Modeling noise and error correction for Majorana-based quantum computing,* Quantum **2**, 88 (2018).

[26] J. Alicea, *New directions in the pursuit of Majorana fermions in solid state systems,* Rep. Prog. Phys. **75**, 076501 (2012).

[27] M. Leijnse and K. Flensberg, *Introduction to topological superconductivity and Majorana fermions,* Semicond. Sci. Technol. **27**, 124003 (2012).

[28] C. Beenakker, *Search for Majorana Fermions in Superconductors,* Annu. Rev. Condens. Matter Phys. **4**, 113 (2013).

[29] M. Sato and S. Fujimoto, *Majorana Fermions and Topology in Superconductors,* J. Phys. Soc. Jpn. **85**, 072001 (2016).

[30] T. Mizushima, Y. Tsutsumi, T. Kawakami, M. Sato, M. Ichioka, and K. Machida, *Symmetry-Protected Topological Superfluids and Superconductors– From the Basics to ^{3}He–,* J. Phys. Soc. Jpn. **85**, 022001 (2016).

[31] V. Mourik, K. Zuo, S. M. Frolov, S. R. Plissard, E. P. A. M. Bakkers, and L. P. Kouwenhoven, *Signatures of Majorana Fermions in Hybrid Superconductor-Semiconductor Nanowire Devices,* Science **336**, 1003 (2012).

[32] M. T. Deng, C. L. Yu, G. Y. Huang, M. Larsson, P. Caroff, and H. Q. Xu, *Anomalous Zero-Bias Conductance Peak in a Nb-InSb Nanowire-Nb Hybrid Device,* Nano Letters **12**, 6414 (2012).

[33] A. Das, Y. Ronen, Y. Most, Y. Oreg, M. Heiblum, and H. Shtrikman, *Zero-bias peaks and splitting in an Al-InAs nanowire topological superconductor as a signature of Majorana fermions,* Nat. Phys. **8**, 887 (2012).

[34] E. Prada, P. San-Jose, M. W. A. de Moor, A. Geresdi, E. J. H. Lee, J. Klinovaja, D. Loss, J. Nygård, R. Aguado, and L. P. Kouwenhoven, *From Andreev to Majorana bound states in hybrid superconductor–semiconductor nanowires,* Nature Reviews Physics **2**, 575 (2020).

[35] I. Affleck, A. Rahmani, and D. Pikulin, *Majorana-Hubbard model on the square lattice,* Phys. Rev. B **96**, 125121 (2017).

[36] A. Rahmani, D. Pikulin, and I. Affleck, *Phase diagrams of Majorana-Hubbard ladders,* Phys. Rev. B **99**, 085110 (2019).

[37] Y. Hu and C. L. Kane, *Fibonacci Topological Superconductor,* Phys. Rev. Lett. **120**, 066801 (2018).

[38] C.-K. Chiu, D. I. Pikulin, and M. Franz, *Strongly interacting Majorana fermions,* Phys. Rev. B **91**, 165402 (2015).

[39] A. Rahmani and M. Franz, *Interacting Majorana fermions,* Reports on Progress in Physics **82**, 084501 (2019).

[40] J. Maldacena and D. Stanford, *Remarks on the Sachdev-Ye-Kitaev model,* Phys. Rev. D **94**, 106002 (2016).

[41] N. E. Bonesteel, L. Hormozi, G. Zikos, and S. H. Simon, *Braid Topologies for Quantum Computation,* Phys. Rev. Lett. **95**, 140503 (2005).

[42] N. Read and E. Rezayi, *Beyond paired quantum Hall states: Parafermions and incompressible states in the first excited Landau level,* Phys. Rev. B **59**, 8084 (1999).

[43] N. R. Cooper, N. K. Wilkin, and J. M. F. Gunn, *Quantum Phases of Vortices in Rotating Bose-Einstein Condensates,* Phys. Rev. Lett. **87**, 120405 (2001).

[44] R. S. K. Mong, D. J. Clarke, J. Alicea, N. H. Lindner, P. Fendley, C. Nayak, Y. Oreg, A. Stern, E. Berg, K. Shtengel, and M. P. A. Fisher, *Universal Topological Quantum Computation from a Superconductor-Abelian Quantum Hall Heterostructure,* Phys. Rev. X **4**, 011036 (2014).

[45] I. Lesanovsky and H. Katsura, *Interacting Fibonacci anyons in a Rydberg gas,* Phys. Rev. A **86**, 041601 (2012).

[46] C. M. Bender and S. Boettcher, *Real Spectra in Non-Hermitian Hamiltonians Having $\mathcal{PT}$ Symmetry,* Phys. Rev. Lett. **80**, 5243 (1998).

[47] M. S. Rudner and L. S. Levitov, *Topological Transition in a Non-Hermitian Quantum Walk,* Phys. Rev. Lett. **102**, 065703 (2009).

[48] K. Esaki, M. Sato, K. Hasebe, and M. Kohmoto, *Edge states and topological phases in non-Hermitian systems,* Phys. Rev. B **84**, 205128 (2011).

[49] H. Shen, B. Zhen, and L. Fu, *Topological Band Theory for Non-Hermitian Hamiltonians,* Phys. Rev. Lett. **120**, 146402 (2018).

[50] K. Kawabata, S. Higashikawa, Z. Gong, Y. Ashida, and M. Ueda, *Topological unification of time-reversal and particle-hole symmetries in non-Hermitian physics,* Nature Communications **10**, 297 (2019).

[51] J. Preskill, *Lecture Notes for Physics 219: Quantum Computation —Part III: Topological Quantum Computation,* (2019).

[52] R. Koenig, G. Kuperberg, and B. W. Reichardt, *Quantum computation with Turaev-Viro codes,* Ann. Phys. **325**, 2707 (2010).

[53] M. H. Freedman, J. Gukelberger, M. B. Hastings, S. Trebst, M. Troyer, and Z. Wang, *Galois conjugates of topological phases,* Phys. Rev. B **85**, 045414 (2012).

[54] E. Ardonne, J. Gukelberger, A. W. W. Ludwig, S. Trebst, and M. Troyer, *Microscopic models of interacting Yang–Lee anyons,* New J. Phys. **13**, 045006 (2011).

[55] J. K. Pachos, *Introduction to Topological Quantum Computation* (Cambridge University Press, 2012).

[56] A. Kitaev, *Fault-tolerant quantum computation by anyons,* Annals of Physics **303**, 2 (2003).

[57] A. P. Schnyder, S. Ryu, A. Furusaki, and A. W. W. Ludwig, *Classification of topological insulators and superconductors in three spatial dimensions,* Phys. Rev. B **78**, 195125 (2008).

[58] Y. Hatsugai, *Chern number and edge states in the integer quantum Hall effect,* Phys. Rev. Lett. **71**, 3697 (1993).

[59] V. G. Turaev, *Axioms for topological quantum field theories,* Annales de la Faculté des sciences de Toulouse : Mathématiques **Ser. 6, 3**, 135 (1994).

[60] E. Majorana and L. Maiani, *A symmetric theory of electrons and positrons,* in Ettore Majorana Scientific Papers: On occasion of the centenary of his birth, edited by G. F. Bassani (Springer Berlin Heidelberg, Berlin, Heidelberg, 2006) pp. 201–233.

[61] E. Majorana, *Teoria simmetrica dell'elettrone e del positrone,* Il Nuovo Cimento (1924-1942) **14**, 171 (2008).

[62] J. C. Y. Teo and C. L. Kane, *Topological defects and gapless modes in insulators and superconductors,* Phys. Rev. B **82**, 115120 (2010).

[63] K. Shiozaki and M. Sato, *Topology of crystalline insulators and superconductors,* Phys. Rev. B **90**, 165114 (2014).

[64] S. Fujimoto, *Topological order and non-Abelian statistics in noncentrosymmetric s-wave superconductors,* Phys. Rev. B **77**, 220501 (2008).

[65] M. Sato, Y. Takahashi, and S. Fujimoto, *Non-Abelian Topological Order in s-Wave Superfluids of Ultracold Fermionic Atoms,* Phys. Rev. Lett. **103**, 020401 (2009).

[66] M. Sato, Y. Takahashi, and S. Fujimoto, *Non-Abelian topological orders and Majorana fermions in spin-singlet superconductors,* Phys. Rev. B **82**, 134521 (2010).

[67] L. Fu and C. L. Kane, *Superconducting Proximity Effect and Majorana Fermions at the Surface of a Topological Insulator,* Phys. Rev. Lett. **100**, 096407 (2008).

[68] T. Machida, Y. Sun, S. Pyon, S. Takeda, Y. Kohsaka, T. Hanaguri, T. Sasagawa, and T. Tamegai, *Zero-energy vortex bound state in the superconducting topological surface state of Fe(Se,Te),* Nature Materials **18**, 811 (2019).

[69] D. Wang, L. Kong, P. Fan, H. Chen, S. Zhu, W. Liu, L. Cao, Y. Sun, S. Du, J. Schneeloch, R. Zhong, G. Gu, L. Fu, H. Ding, and H.-J. Gao, *Evidence for Majorana bound states in an iron-based superconductor,* Science **362**, 333 (2018).

[70] T. Karzig, Y. Oreg, G. Refael, and M. H. Freedman, *Universal Geometric Path to a Robust Majorana Magic Gate,* Phys. Rev. X **6**, 031019 (2016).

[71] T. Sanno, S. Miyazaki, T. Mizushima, and S. Fujimoto, *Ab initio simulation of non-Abelian braiding statistics in topological superconductors*, Phys. Rev. B **103**, 054504 (2021).

[72] C. S. Amorim, K. Ebihara, A. Yamakage, Y. Tanaka, and M. Sato, *Majorana braiding dynamics in nanowires,* Phys. Rev. B **91**, 174305 (2015).

[73] Y. Tanaka, T. Sanno, T. Mizushima, and S. Fujimoto, *Manipulation of Majorana-Kramers qubit and its tolerance in time-reversal invariant topological superconductor*, Phys. Rev. B **106**, 014522 (2022).

[74] T. Zhou, M. C. Dartiailh, K. Sardashti, J. E. Han, A. Matos-Abiague, J. Shabani, and I. Žutić, *Fusion of Majorana bound states with mini-gate control in two-dimensional systems,* Nature Communications **13**, 1738 (2022).

[75] F. Harper, A. Pushp, and R. Roy, *Majorana braiding in realistic nanowire Y-junctions and tuning forks,* Phys. Rev. Research **1**, 033207 (2019).

[76] L. Hormozi, G. Zikos, N. E. Bonesteel, and S. H. Simon, *Topological quantum compiling,* Phys. Rev. B **75**, 165310 (2007).

[77] P. H. Bonderson, *Non-Abelian Anyons and Interferometry*, Ph.D. thesis, California Institute of Technology (2007).

[78] K. Gawędzki and A. Kupiainen, *G/H conformal field theory from gauged WZW model,* Physics Letters B **215**, 119 (1988).

[79] D. Karabali, Q.-H. Park, H. J. Schnitzer, and Z. Yang, *A GKO construction based on a path integral formulation of gauged Wess-Zumino-Witten actions,* Physics Letters B **216**, 307 (1989).

[80] J. Slingerland and F. Bais, *Quantum groups and non-Abelian braiding in quantum Hall systems,* Nuclear Physics B **612**, 229 (2001).

[81] H. Terashima and M. Ueda, *nonunitary quantum circuit,* Int. J. Quantum Inform. **3**, 633 (2005).

[82] N. Usher, M. J. Hoban, and D. E. Browne, *Nonunitary quantum computation in the ground space of local Hamiltonians,* Phys. Rev. A **96**, 032321 (2017).

[83] L. Piroli and J. I. Cirac, *Quantum Cellular Automata, Tensor Networks, and Area Laws,* Phys. Rev. Lett. **125**, 190402 (2020).

[84] C. Zheng, *Universal quantum simulation of single-qubit nonunitary operators using duality quantum algorithm,* Sci. Rep. **11**, 3960 (2021).

[85] A. Belavin, A. Polyakov, and A. Zamolodchikov, *Infinite conformal symmetry in two-dimensional quantum field theory,* Nuclear Physics B **241**, 333 (1984).

[86] P. Francesco, P. Mathieu, and D. Sénéchal, *Conformal field theory* (Springer Science & Business Media, 2012).

[87] J. Cardy, *Conformal field theory and statistical mechanics,* Exact Methods in Lowdimensional Statistical Physics and Quantum Computing (Oxford University Press, Oxford, 2010) , 65 (2008).

[88] H. W. J. Blöte, J. L. Cardy, and M. P. Nightingale, *Conformal invariance, the central charge, and universal finite-size amplitudes at criticality,* Phys. Rev. Lett. **56**, 742 (1986).

[89] I. Affleck, *Universal term in the free energy at a critical point and the conformal anomaly,* Phys. Rev. Lett. **56**, 746 (1986).

[90] F. C. Alcaraz, M. N. Barber, and M. T. Batchelor, *Conformal invariance and the spectrum of the XXZ chain,* Phys. Rev. Lett. **58**, 771 (1987).

[91] K. G. Wilson, *The renormalization group and critical phenomena,* Rev. Mod. Phys. **55**, 583 (1983).

[92] A. B. Zamolodchikov, *Irreversibility of the Flux of the Renormalization Group in a 2D Field Theory,* Jetp Letters **43**, 565 (1986).

[93] E. Witten, *Quantum field theory and the Jones polynomial,* Communications in Mathematical Physics **121**, 351 (1989).

[94] J. C. Ward, *An Identity in Quantum Electrodynamics,* Phys. Rev. **78**, 182 (1950).

[95] Y. Takahashi, *On the generalized ward identity,* Il Nuovo Cimento **6**, 371 (1957).

[96] E. Noether, *Invariant variation problems,* Transport Theory and Statistical Physics **1**, 186 (1971).

[97] A. E. Ferdinand and M. E. Fisher, *Bounded and Inhomogeneous Ising Models. I. Specific-Heat Anomaly of a Finite Lattice,* Phys. Rev. **185**, 832 (1969).

[98] V. G. Kac, *Contravariant form for infinite-dimensional Lie algebras and superalgebras,* in *Group Theoretical Methods in Physics*, edited by W. Beiglböck, A. Böhm, and E. Takasugi (Springer Berlin Heidelberg, Berlin, Heidelberg, 1979) pp. 441–445.

[99] B. L. Feigin and D. B. Fuchs, *Invariant skew-symmetric differential operators on the line and Verma modules over the Virasoro algebra,* Funktsional'nyi Analiz i ego Prilozheniya **16**, 47 (1982).

[100] B. L. Feigin and D. B. Fuchs, *Verma modules over the Virasoro algebra,* in *Topology* (Springer, 1984) pp. 230–245.

[101] L. Onsager, *Crystal Statistics. I. A Two-Dimensional Model with an Order-Disorder Transition,* Phys. Rev. **65**, 117 (1944).

[102] B. Kaufman and L. Onsager, *Crystal Statistics. III. Short-Range Order in a Binary Ising Lattice,* Phys. Rev. **76**, 1244 (1949).

[103] Y. Nambu, *A Note on the Eigenvalue Problem in Crystal Statistics,* Progress of Theoretical Physics **5**, 1 (1950).

[104] D. Friedan, Z. Qiu, and S. Shenker, *Superconformal invariance in two dimensions and the tricritical Ising model,* Physics Letters B **151**, 37 (1985).

[105] I. Affleck, M. Oshikawa, and H. Saleur, *Boundary critical phenomena in the three-state Potts model,* Journal of Physics A: Mathematical and General **31**, 5827 (1998).

[106] V. V. BAZHANOV and N. YU. RESHETIKHIN, *Critical RSOS Models and Conformal Field Theory,* International Journal of Modern Physics A **04**, 115 (1989).

[107] G. Feverati and P. A. Pearce, *Critical RSOS and minimal models: fermionic paths, Virasoro algebra and fields,* Nuclear Physics B **663**, 409 (2003).

[108] C. N. Yang and T. D. Lee, *Statistical Theory of Equations of State and Phase Transitions. I. Theory of Condensation,* Phys. Rev. **87**, 404 (1952).

[109] T. D. Lee and C. N. Yang, *Statistical Theory of Equations of State and Phase Transitions. II. Lattice Gas and Ising Model,* Phys. Rev. **87**, 410 (1952).

[110] M. E. Fisher, *Yang-Lee Edge Singularity and ϕ^3 Field Theory,* Phys. Rev. Lett. **40**, 1610 (1978).

[111] J. L. Cardy, *Conformal Invariance and the Yang-Lee Edge Singularity in Two Dimensions,* Phys. Rev. Lett. **54**, 1354 (1985).

[112] C. Itzykson, H. Saleur, and J.-B. Zuber, *Conformal Invariance of Nonunitary 2d-Models,* Europhys. Lett. **2**, 91 (1986).

[113] G. von Gehlen, *Critical and off-critical conformal analysis of the Ising quantum chain in an imaginary field,* J. Phys. A: Math. Gen. **24**, 5371 (1991).

[114] B.-B. Wei and R.-B. Liu, *Lee-Yang Zeros and Critical Times in Decoherence of a Probe Spin Coupled to a Bath,* Phys. Rev. Lett. **109**, 185701 (2012).

[115] X. Peng, H. Zhou, B.-B. Wei, J. Cui, J. Du, and R.-B. Liu, *Experimental Observation of Lee-Yang Zeros,* Phys. Rev. Lett. **114**, 010601 (2015).

[116] D. A. Huse, *Exact exponents for infinitely many new multicritical points,* Phys. Rev. B **30**, 3908 (1984).

[117] G. E. Andrews, R. J. Baxter, and P. J. Forrester, *Eight-vertex RSOS model and generalized Rogers-Ramanujan-type identities,* Journal of Statistical Physics **35**, 193 (1984).

[118] B. Widom, *Surface Tension and Molecular Correlations near the Critical Point,* The Journal of Chemical Physics **43**, 3892 (1965).

[119] A. Patashinskii and V. Pokrovskii, *Behavior of ordered systems near the transition point,* Sov. Phys. JETP **23**, 292 (1966).

[120] L. P. Kadanoff, *Scaling laws for ising models near T_c,* Physics Physique Fizika **2**, 263 (1966).

[121] J. Polchinski, *Scale and conformal invariance in quantum field theory,* Nuclear Physics B **303**, 226 (1988).

[122] J. L. Cardy, *Is there a c-theorem in four dimensions?* Physics Letters B **215**, 749 (1988).

[123] H. Casini and M. Huerta, *A finite entanglement entropy and the c-theorem,* Physics Letters B **600**, 142 (2004).

[124] H. Casini and M. Huerta, *Renormalization group running of the entanglement entropy of a circle,* Phys. Rev. D **85**, 125016 (2012).

[125] H. Casini, E. Testé, and G. Torroba, *Markov Property of the Conformal Field Theory Vacuum and the a Theorem,* Phys. Rev. Lett. **118**, 261602 (2017).

[126] P. Calabrese and J. Cardy, *Entanglement entropy and quantum field theory,* J. Stat. Mech.: Theory Exp. **2004**, P06002 (2004).

[127] P. Calabrese and J. Cardy, *Entanglement entropy and conformal field theory,* J. Phys. A **42**, 504005 (2009).

[128] S. Ryu and T. Takayanagi, *Holographic Derivation of Entanglement Entropy from the anti–de Sitter Space/Conformal Field Theory Correspondence,* Phys. Rev. Lett. **96**, 181602 (2006).

[129] M. Srednicki, *Entropy and area,* Phys. Rev. Lett. **71**, 666 (1993).

[130] G. Vidal, J. I. Latorre, E. Rico, and A. Kitaev, *Entanglement in Quantum Critical Phenomena,* Phys. Rev. Lett. **90**, 227902 (2003).

[131] M. M. Wolf, *Violation of the Entropic Area Law for Fermions,* Phys. Rev. Lett. **96**, 010404 (2006).

[132] C. Holzhey, F. Larsen, and F. Wilczek, *Geometric and renormalized entropy in conformal field theory,* Nuclear Physics B **424**, 443 (1994).

[133] I. Affleck and A. W. W. Ludwig, *Universal noninteger "ground-state degeneracy" in critical quantum systems,* Phys. Rev. Lett. **67**, 161 (1991).

[134] B. Nienhuis, M. Campostrini, and P. Calabrese, *Entanglement, combinatorics and finite-size effects in spin chains,* Journal of Statistical Mechanics: Theory and Experiment **2009**, P02063 (2009).

[135] D. Bianchini, O. A. Castro-Alvaredo, and B. Doyon, *Entanglement entropy of non-unitary integrable quantum field theory,* Nucl. Phys. B **896**, 835 (2015).

[136] D. Bianchini, O. Castro-Alvaredo, B. Doyon, E. Levi, and F. Ravanini, *Entanglement entropy of non-unitary conformal field theory,* J. Phys. A **48**, 04FT01 (2014).

[137] R. Couvreur, J. L. Jacobsen, and H. Saleur, *Entanglement in Nonunitary Quantum Critical Spin Chains,* Phys. Rev. Lett. **119**, 040601 (2017).

[138] P.-Y. Chang, J.-S. You, X. Wen, and S. Ryu, *Entanglement spectrum and entropy in topological non-Hermitian systems and nonunitary conformal field theory,* Phys. Rev. Res. **2**, 033069 (2020).

[139] P. Dorey, C. Dunning, and R. Tateo, *Supersymmetry and the spontaneous breakdown of $\mathcal{PT}$ symmetry,* Journal of Physics A: Mathematical and General **34**, L391 (2001).

[140] D. C. Brody, *Biorthogonal quantum mechanics,* Journal of Physics A: Mathematical and Theoretical **47**, 035305 (2013).

[141] T. Curtright and L. Mezincescu, *Biorthogonal quantum systems,* Journal of Mathematical Physics **48**, 092106 (2007).

[142] O. A. Castro-Alvaredo and A. Fring, *A spin chain model with non-Hermitian interaction: the Ising quantum spin chain in an imaginary field,* Journal of Physics A: Mathematical and Theoretical **42**, 465211 (2009).

[143] A. M. Tsvelik, *New fermionic description of quantum spin liquid state,* Phys. Rev. Lett. **69**, 2142 (1992).

[144] M. Cheng, R. M. Lutchyn, V. Galitski, and S. Das Sarma, *Splitting of Majorana-Fermion Modes due to Intervortex Tunneling in a $p_x + ip_y$ Superconductor,* Phys. Rev. Lett. **103**, 107001 (2009).

[145] T. Mizushima and K. Machida, *Splitting and oscillation of Majorana zero modes in the p-wave BCS-BEC evolution with plural vortices,* Phys. Rev. A **82**, 023624 (2010).

[146] J. Alicea, Y. Oreg, G. Refael, F. von Oppen, and M. P. A. Fisher, *Non-Abelian statistics and topological quantum information processing in 1D wire networks,* Nat. Phys. **7**, 412 (2011).

[147] P. Bonderson, M. Freedman, and C. Nayak, *Measurement-Only Topological Quantum Computation,* Phys. Rev. Lett. **101**, 010501 (2008).

[148] S. Vijay and L. Fu, *Teleportation-based quantum information processing with Majorana zero modes,* Phys. Rev. B **94**, 235446 (2016).

[149] M. G. Yamada, T. Sanno, M. O. Takahashi, Y. Akagi, H. Suwa, S. Fujimoto, and M. Udagawa, *Matrix Product Renormalization Group: Potential Universal Quantum Many-Body Solver,* arXiv preprint arXiv:2212.13267 (2022)